Fig. 5. Activation of IFN-β gene by NS5B is mediated through the TLR3 signaling pathway. (A) Down-regulation of IFN-β mRNA by transfection of TLR3 siRNA. PH/NS5B cells were transfected with dsRNA duplexes targeting TLR3, TLR4, or luciferase GL2. After 3 days, the expression levels of TLR3, TLR4, IFN-β, and GAPDH mRNAs were examined by RT-PCR. (B) Growth curve of PH/NS5B cells transfected with siRNAs. After 2 days of transfection, the proliferation kinetics of PH/NS5B cells transfected with GL2 (circles), TLR3 (squares), and TLR4 (triangles) siRNAs were analyzed as indicated in Fig. 1F. (C) BrdUrd incorporation analysis of PH/NS5B cells transfected with GL2, TLR3, and TLR4 siRNAs. After 2 days of transfection, the cells were synchronized, and cell cycle progression was analyzed as indicated in Fig. 1D.

retrovirus pCXpur encoding TLR3 or pCXpur as a negative control, yielding cells stably expressing TLR3 and control HEK293 cells. The expression of NS5B or TLR3 was confirmed by Western blot analysis (Fig. 6A). We then performed a dual-luciferase reporter assay using an IFN-β gene promoter. The results revealed that the luciferase activity was enhanced in only the HEK293 cells stably expressing both NS5B and TLR3 (Fig. 6B). This suggests that TLR3 mediates NS5B's induction of IFN-β. However, since the enhancement of luciferase activity was approximately two-fold, we failed to detect the enhancement of the mRNA expression levels for IFN-β and one of its target genes, ISG56 (data not shown). To accurately assess the

enhancement, high expression levels of NS5B and TLR3 in HEK293 cells will be needed.

The RIG-I-mediated signaling pathway is not implicated in the induction of IFN-β in PH/NS5B cells

Recently, RIG-I, a cellular DExD/H box helicase, was found to be a double-stranded RNA (dsRNA) binding protein that functions independently of TLR3 to induce IFN-β in response to viral infection (Yoneyama et al., 2004). Since another recent study showed that both the TLR3- and RIG-I-mediated signaling pathways are functional in PH5CH8 cells (Li et al., 2005a, 2005b), we examined whether or not the RIG-I-mediated signaling pathway is involved in NS5B's induction of IFN-β. First, PH/NS5B and PH/Ctr cells were infected with retrovirus pCXpur encoding myc-tagged RIG-IC, a dominant negative inhibitor of RIG-I harboring only the helicase domain but not the two N-terminal CARD domains (Yoneyama et al., 2004), or pCXpur as a negative control. Cells that stably expressed myc-tagged RIG-IC were thus obtained. The expression of myc-
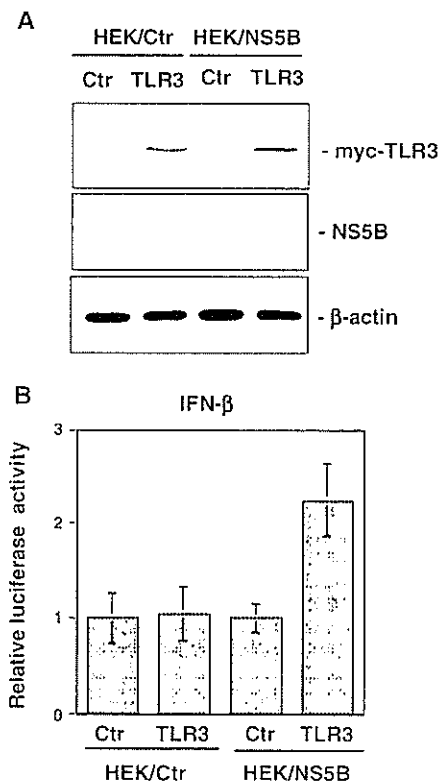

Fig. 6. Ectopic expression of TLR3 enhances the IFN-β gene promoter in only the HEK293 cells stably expressing NS5B. (A) Expression of TLR3 and NS5B in HEK293 cells introduced by retrovirus-mediated gene transfer. Western blot analysis of HEK/Ctr or HEK/NS5B cells infected with pCXpur retrovirus encoding myc-tagged TLR3 was performed. The pCXpur retrovirus was used as a control infection. Anti-myc, anti-NS5B, and anti-β-actin antibodies were used for the immunoblotting analysis. (B) Dual luciferase reporter assay of the IFN-β gene promoter. The cells shown in panel A were transfected with pIFN-β(-125)-Luc, and the dual luciferase assay was performed as described previously (Dansako et al., 2003). Data are means ± SD from three independent triplicate experiments.
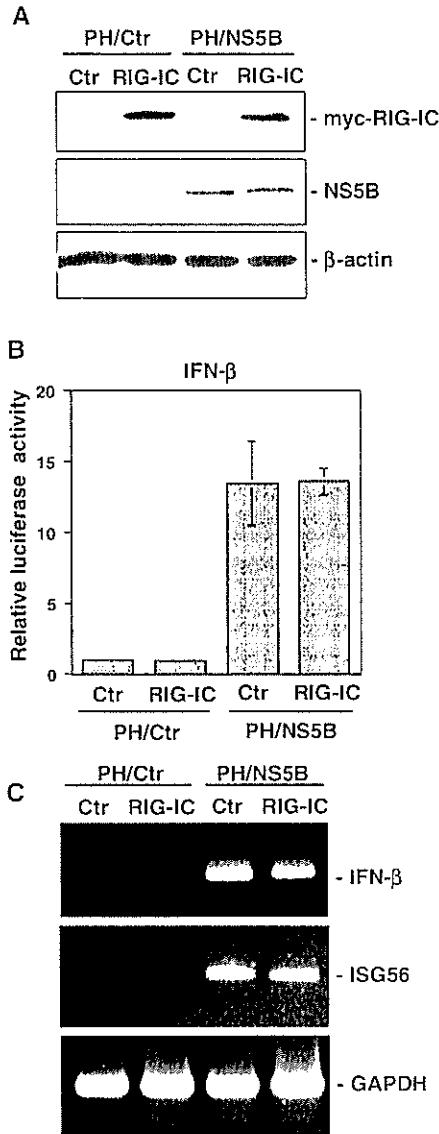
A

B

C

Fig. 7. Induction of IFN-β by NS5B is not mediated through the RIG-I signaling pathway. (A) Expression of RIG-IC and NS5B in PH5CH8 cells introduced by retrovirus-mediated gene transfer. Western blot analysis of PH/ Ctr or PH/NS5B cells infected with pCXpur retrovirus encoding myc-tagged RIG-IC was performed. The pCXpur retrovirus was used as a control infection. Anti-myc, anti-NS5B, and anti-β-actin antibodies were used for the immunoblotting analysis. (B) Dual luciferase reporter assay of the IFN-β gene promoter. The cells shown in panel A were transfected with pIFN-β(-125)-Luc, and the dual luciferase assay was performed as indicated in Fig. 6B. (C) RT-PCR analysis of IFN-β and ISG56 mRNAs. The total RNAs were extracted from the cells shown in panel A and subjected to RT-PCR analysis using primer sets for IFN-β (341 bp), ISG56 (320 bp), and GAPDH (587 bp).

The results revealed that the enhancement of luciferase activity in PH/NS5B cells was not suppressed regardless of RIG-IC expression (Fig. 7B). Furthermore, the mRNA expression levels for IFN-β and one of its target genes, ISG56, were also unchanged by the expression of RIG-IC (Fig. 7C). These results suggest that NS5B's induction of IFN-β is not mediated through the RIG-I signaling pathway.

NS5B does not interact with TLR3 adaptor protein

Since we showed that NS5B's induction of IFN-β was mediated through the TLR3 but not the RIG-I signaling pathway, we further examined the mechanism underlying IFN-β induction by testing the possibility of interaction between NS5B and the TLR3 adaptor protein TRIF (Yamamoto et al., 2002). We prepared HEK/NS5B cells stably expressing myc-tagged NS5A or myc-tagged TRIF and examined whether or not NS5B interacts with TRIF by an immunoprecipitation method following Western blot analysis. The results clearly showed that NS5B and myc-tagged NS5A were co-immunoprecipitated by anti-myc antibody as reported previously (Shirota et al., 2002). However, co-immunoprecipitation of NS5B and myc-tagged TRIF was clearly not observed (Fig. 8). This result suggests that the activation of the TLR3 signaling pathway by NS5B occurs through one or more factors other than TRIF.

Induction of IFN-β depends on RNA-dependent RNA polymerase (RdRp) activity of NS5B

Since dsRNA, an intermediate of viral replication, is known as a natural ligand for the activation of TLR3 (Alexopoulou et
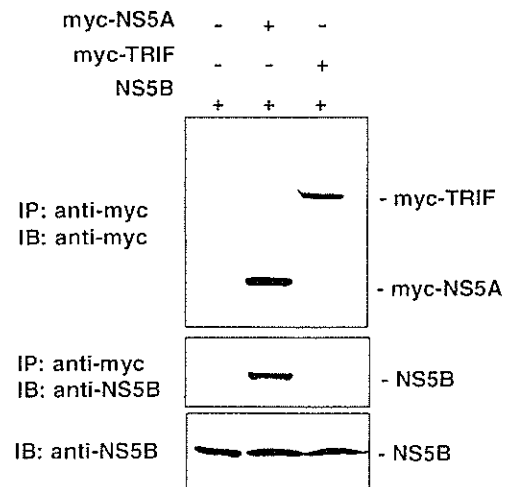

Fig. 8. NS5B does not interact with TRIF. HEK/NS5B cells were infected with pCXpur retrovirus encoding myc-tagged NS5A (middle lane) or myc-tagged TRIF (right lane). pCXpur retrovirus was used as a control infection (left lane). Cell lysate was immunoprecipitated (IP) with anti-myc antibody-conjugated agarose beads. The immunoprecipitates were resolved by SDS-PAGE, and anti-myc (upper panel) and anti-NS5B (middle panel) antibodies were used for the immunoblotting (IB) analysis. To confirm the expression level of NS5B, cell lysates were subjected to immunoblotting analysis using anti-NS5B antibody (lower panel).

tagged RIG-IC was confirmed by Western blot analysis (Fig. 7A). Using PH/Ctr cells stably expressing myc-tagged RIG-IC, we confirmed that IFN-β production was markedly suppressed after infection with Sendai virus (data not shown), as initially observed in Newcastle disease virus infection (Yoneyama et al. 2004). This indicates that RIG-IC functions as a dominant negative inhibitor of RIG-I in PH5CH8 cells. We then performed a dual-luciferase reporter assay using an *IFN-β* gene promoter.

al., 2001; Takeda et al., 2003), we next examined whether or not the induction of IFN-β in human hepatocytes expressing NS5B (591 amino acids; amino acids 2420 to 3010 in the HCV-1b genotype) (Kato et al., 1990) depends on NS5B's RdRp activity. Since this activity is already well characterized (Hagedorn et al., 2000), we constructed several NS5B mutants to evaluate this subject (Fig. 9A). One is the substitution mutant G2736V of the GDD motif (amino acids 2736–8) located in the catalytic site, and the other is the deletion mutant Δ2575–7 (R2753T, K2754S, and Δ2575–7) at the priming and interrogation sites, all of which are essential for NS5B's RdRp activity (Behrens et al., 1996; Bressanelli et al., 2002). We also constructed three carboxyl-truncated forms (ΔC21, ΔC56, and ΔC97, lacking 21, 56, and 97 amino acids, respectively) of NS5B. These truncated mutants of NS5B lack the last 21 hydrophobic amino acids, which are necessary and sufficient to target NS5B to the cytosolic side of the endoplasmic reticulum (ER) membrane (Schmidt-Mende et al., 2001, Yamashita et al., 1998). Although ΔC21 and ΔC56, but not ΔC97, possess RdRp activity in vitro, ΔC56 shows higher RdRp activity than ΔC21 because only the latter possesses a regulatory motif inhibiting RNA binding and polymerase activity (Leveque et al., 2003). We prepared PH5CH8 cells stably expressing these NS5B mutants and then performed cell cycle analysis using these
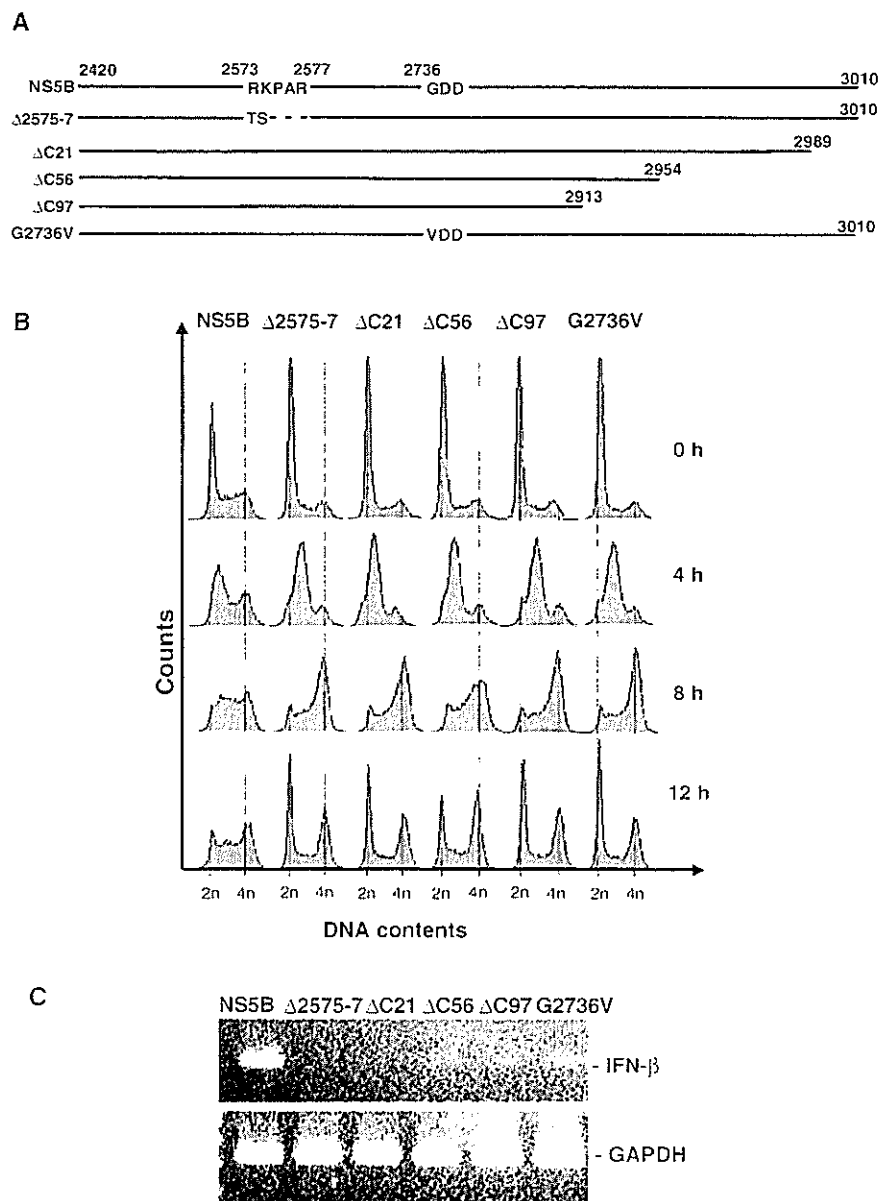

Fig. 9. The RdRp activity of NS5B anchoring on ER membrane is required for induction of IFN-β and following the delay of S phase progression. (A) Schematic presentation of the NS5B mutants used. Only amino acid sequences in the mutated regions of NS5B are indicated. (B) Cell cycle analysis of PH/NS5B and PH5CH8 cells expressing NS5B mutants. Cell cycle distribution was analyzed as described in Fig. B. (C) RT-PCR analysis of IFN-β mRNA in PH/NS5B and PH5CH8 cells expressing NS5B mutants. RT-PCR analysis was performed as described in Fig. 3A.

prepared cells. The results revealed no effect on S phase progression in the PH5CH8 cells expressing NS5B mutants (Fig. 9B), although PH5CH8 cells expressing ΔC56 showed a slight delay of S phase progression. Induction of IFN-β mRNA was also not observed in the PH5CH8 cells expressing NS5B mutants (Fig. 9C). These results revealed that the delay of S phase progression and the induction of IFN-β depend on the RdRp activity of NS5B, and these effects are coupled with ER membrane anchorage of NS5B in cells.

To examine the activation of IRF3, a factor specifically induced by stimulated TLR3 or TLR4, by the expression of NS5B and its mutants, we performed a dual-luciferase reporter assay using a synthetic promoter having five repeats of the consensus ISRE, which was the same as the IRF3 target sequence in the *IFN-β* gene promoter (Fig. 10A) and an intrinsic *IFN-β* gene promoter (Fig. 10B). The results showed that the luciferase activity was enhanced approximately five-fold (Fig. 10A) and eight-fold (Fig. 10B) only in PH/NS5B cells,
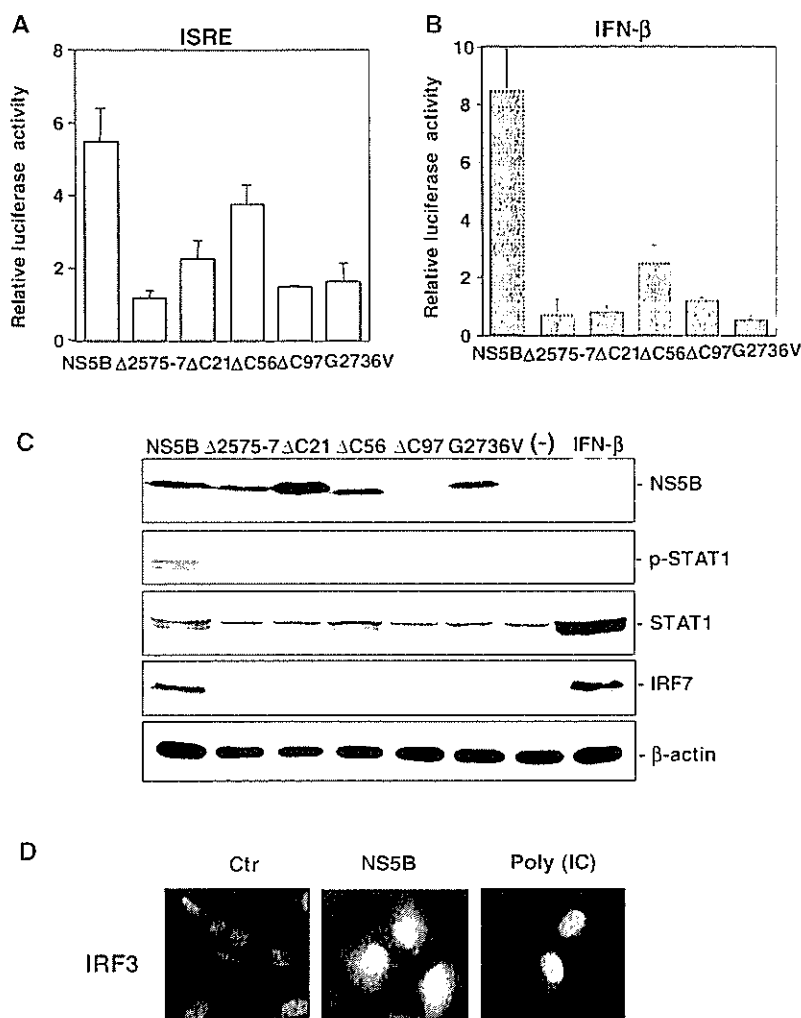

Fig. 10. NS5B full form is required for activation of IRF3 target sequences and IFN-β signaling pathway. (A) Dual luciferase reporter assay toward IRF3 target sequences. PH5CH8 cells were transfected with the pISRE-Luc (Stratagene) and pCXbsr encoding NS5B or its mutant, and the dual luciferase assay was performed as indicated in Fig. 6B. The lysates of cells transfected with pCXbsr were used as a control. (B) Dual luciferase reporter assay of the IFN-β gene promoter. Dual luciferase assay was performed as described in panel A except using pIFN-β(-125)-Luc instead of pISRE-Luc. (C) Western blot analysis of the components involved in the IFN-β signaling pathway. The lysates of PH/NS5B and PH5CH8 cells expressing NS5B mutants were subjected to immunoblotting using anti-NS5B, anti-p-STAT1(Y701), anti-STAT1, anti-IRF7, and anti-β-actin antibodies. PH5CH8 cells treated with or without IFN-β (500 IU/ml for 24 h) were also analyzed as a control. (D) Subcellular distribution of endogenous IRF3. PH/Ctr and PH/NS5B cells were processed and stained with anti-IRF3 antibody and an FITC-conjugated secondary antibody. PH5CH8 cells treated with poly (IC) were also used as a positive control.

suggesting that IRF3 is activated by the NS5B full form. Interestingly, however, luciferase activity was enhanced approximately four-fold (Fig. 10A) and three-fold (Fig. 10B) in PH5CH8 cells expressing ΔC56, although the enhancement was not as great as the five-fold (Fig. 10A) and eight-fold (Fig. 10B) in PH/NS5B cells, respectively. We then examined the phosphorylation status of STAT1 on Y701 and the level of IRF7, one of the downstream targets of the IFN-β signaling pathway (Katze et al., 2002). Western blot analysis revealed marked phosphorylation of STAT1 and IRF7 expression in PH/NS5B cells as well as in PH5CH8 cells treated with IFN-β

(Fig. 10C). Although slight phosphorylation of STAT1 was observed in the PH5CH8 cells expressing ΔC56, IRF7 expression was not observed (Fig. 10C). Unlike PH/NS5B cells and PH5CH8 cells expressing ΔC56, neither the phosphorylation of STAT1 nor the expression of IRF7 was detected in PH5CH8 cells expressing other NS5B mutants. These results indicated that ΔC56 had an extremely low ability to induce IFN-β after activation of TLR3, although ΔC56 was still able to enhance the IRF3 target promoter. To obtain further evidence of the activation of IRF3, we examined the subcellular distribution of endogenous IRF3 in PH/Ctr and PH/NS5B
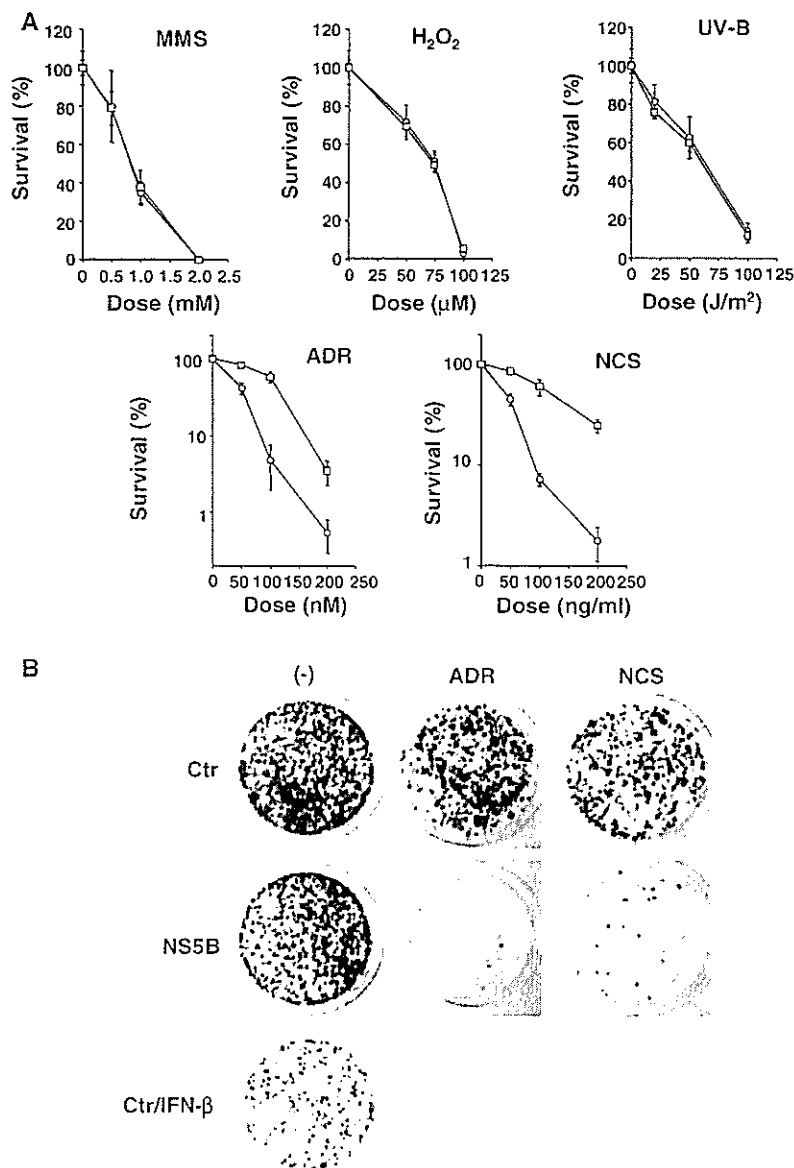
Fig. 11. Sensitivity of PH/NS5B cells against DNA-damaging reagents. (A) Clonogenic assays for PH/Ctr (square) and PH/NS5B (circle) cells after treatment with increasing doses of DNA-damaging reagents. Cells were treated with MMS, H_2O_2, UV-B, ADR, and NCS. Ten days after the treatment, cells were fixed and stained with Coomassie brilliant blue. Only colonies containing >50 cells were scored as being derived from viable clonogenic cells. Data are means ± SD from two independent triplicate experiments. (B) PH/Ctr, PH/NS5B, and IFN-β-treated (20 IU/ml) PH/Ctr cells were treated with ADR (100 nM) or NCS (100 ng/ml). The panels show survived colonies that are stained with Coomassie brilliant blue at 10 days after the treatment.

cells. In PH/Ctr cells, IRF3 was distributed in a perinuclear and/ or cytoplasmic context. However, in PH/NS5B cells as well as PH5CH8 cells treated with poly (IC), IRF3 was distributed to the nucleus, a finding consistent with its activated state (Fig. 10D). Taken together, our findings indicate that the RdRp activity of HCV NS5B anchoring on ER membrane is necessary and sufficient to activate the TLR3 signaling pathway.

PH/NS5B cells are more susceptible than PH/Ctr cells to DNA-damaging reagents

To better understand the effect of IFN-β induction in PH/ NS5B cells, we next examined the susceptibilities of PH/NS5B and PH/Ctr cells against various types of DNA-damaging reagents. A clonogenic assay using PH/NS5B and PH/Ctr cells was performed by treatment with MMS (a DNA alkylating reagent) and H_2O_2 (a DNA oxidative reagent) and by UV-B irradiation, which induces DNA single-strand breaks and/or thymidine dimer formation in DNA. ADR and NCS, which induce DNA double-strand breaks, were also used for the clonogenic assay. As shown in Fig. 11A, PH/NS5B and PH/Ctr cells were susceptible to the MMS treatment, the H_2O_2 treatment, and the UV-B irradiation, and no differences were observed between their susceptibilities. Interestingly, however, PH/NS5B cells were more susceptible than PH/Ctr cells against ADR or NCS treatment (Fig. 11A). These results suggest that PH/NS5B cells are more sensitive than PH/Ctr cells to damage in the form of DNA double-strand breaks. To clarify whether or not IFN-β induction increases the susceptibility against ADR or NCS treatment, we examined the effect of ADR or NCS in PH/ Ctr cells treated with IFN-β. In this treatment, the cells changed to susceptible phenotype against ADR or NCS treatment, as observed in PH/NS5B cells (Fig. 11B). These results suggest that IFN-β induced by NS5B in PH5CH8 cells changes the cells into the hypersensitive phenotype, making them susceptible to DNA damage in the form of double-strand breaks.

Discussion

In the present study, we found that HCV NS5B induced IFN-β in two kinds of immortalized human hepatocyte cell lines, PH5CH8 and NKNT-3. We showed that NS5B's induction of IFN-β was mediated through the TLR3 but not the RIG-I signaling pathway. The induction of IFN-β caused the delay of cell cycle progression through the S phase in these cells. Since it has been generally known that the activation of the TLR3 signaling pathway is caused by dsRNA, a molecular pattern associated with replicating viral genomes, we first obtained data suggesting that dsRNA is generated by NS5B even without replication of the viral genome.

TLRs belong to a family of evolutionarily conserved innate immune recognition molecules, and ten members of the TLR family have been identified in human (Medzhitov '00 Takeda et al., 2003). TLR3 recognizes dsRNA and induces the antiviral immune responses (Alexopoulou et al., 2001 Matsumoto et al., 2002). TLR3 activates transcription factor IRF3 through TRIF, leading to IFN-β production (Oshiumi et

al., 2003; Yamamoto et al., 2002, 2003). We speculated on two possible mechanisms underlying the activation of the TLR3 signaling pathway by NS5B. The first possibility is that protein–protein interaction between NS5B and TRIF is involved in the activation of the TLR3 signaling pathway. However, we failed to obtain evidence of direct interaction between NS5B and TRIF. The second possibility is that the RdRp activity of NS5B contributes to the activation of TLR3. To evaluate this hypothesis, we examined whether or not several NS5B mutants, including carboxyl-truncated mutants or an RdRp activity-defective mutant (G2736V), could induce IFN-β. The experimental data clearly showed that neither the G2736V mutant nor the carboxyl-truncated mutants could induce IFN-β. Therefore, we suggested that NS5B RdRp activity anchoring the ER membrane is critical for the activation of the TLR3 signaling pathway.

The finding that NS5B RdRp activity on the ER membrane was a critical factor for the induction of IFN-β surprised us because we expected that dsRNA, a natural ligand for TLR3, was produced in NS5B-expressing hepatocyte cells without replication of the viral RNA genome. Therefore, we now presume a daring hypothesis: that NS5B can produce dsRNA using cellular RNA as a template on the ER membrane. Since no direct evidence has been found to support this hypothesis at this stage, further experiments are necessary to evaluate this hypothesis. For instance, if possible, the detection of newly synthesized dsRNA in NS5B-expressing cells or the detection of newly synthesized dsRNA by recombinant NS5B using cellular RNA in vitro may become positive evidence. Furthermore, since the formation of a membrane-associated replication complex is a characteristic of positive-stranded RNA viruses, including HCV (Shi et al., 2003), it will also be interesting to examine whether or not the RdRps of the other RNA viruses possess novel activity similar to that observed in this study. At least we recently detected that NS5B derived from an HCV-2a genome designated JFH-1, which produces virus particles infectious for HuH-7 cells (Wakita et al., 2005), also strongly induced IFN-β in PH5CH8 cells (Ikeda et al., unpublished data). In addition, we are not able to completely exclude the possibility that NS5B-encoding RNA, but not NS5B, specifically activates the TLR3 signaling pathway. However, this possibility is unlikely because the G2736V mutant with only one nucleotide substitution could not activate the TLR3 signaling pathway.

Since the activation of the TLR3 signaling pathway in NS5B-expressing PH5CH8 or NKNT-3 cells is considered to be due to a novel function of NS5B, it is important to clarify whether or not this function occurs in the HCV life cycle. Although HCV replicon systems carrying autonomously replicating HCV RNA genomes developed using HuH-7 (Bi it 2000. Ikeda et al 2002 Lc m c al 1999) and HeLa (Zhu c 003) cells have become powerful tools for basic studies of HCV, these systems would not be suitable to prove our hypothesis because the induction of IFN-β by NS5B was not observed in HuH-7 or HeLa cells, in which the TLR3 signaling pathway was suggested to be defective. In fact, it has been recently reported that HuH-7 cells lack a TLR3

response to external dsRNA (Lanford et al., 2003). Therefore, a new HCV replicon system needs to be developed using other human cell lines possessing intact TLR3 signaling pathways. We are currently making a trial to establish an HCV replicon system using PH5CH8 or NKNT-3 cells.

On the other hand, it has been recently found that an HCV serine protease, NS3-4A, can block the phosphorylation and effector action of IRF3 (Foy et al., 2003). This finding using HuH-7 cells suggests that NS3-4A mediates the proteolysis of cellular proteins within an antiviral signaling pathway upstream of IRF3, leading to persistent viral infection. The recently identified TRIF (Li et al., 2005a, 2005b) and RIG-I (Foy et al., 2005) are possible candidates for these cellular proteins. Therefore, it was thought that IFN-β induction by NS5B through the activation of TLR3 might be suppressed by NS3-4A in PH5CH8 cells. In fact, our recent study showed that NS3-4A, in a serine protease activity-dependent manner, suppressed NS5B's activation of the IFN system (Dansako et al., 2005). However, the synergistic induction of IFN-β in PH5CH8 cells co-expressing Core and NS5B was only partially suppressed by NS3-4A, whereas the induction of IFN-β by NS5B only was drastically suppressed by NS3-4A (Dansako et al., 2005). We speculate that a biological implication of this phenomenon is that HCV proteins contribute to the maintenance of a low steady state of the virus by controlling the expression level of IFN-β in the infected cells.

In addition to the delay of cell cycle progression through the S phase, enhanced susceptibility to DNA-damaging reagents was found in NS5B-expressing PH5CH8 cells. This phenomenon was attributed to IFN-β induced by NS5B. Further characterization of this phenomenon may contribute to the understanding of IFN-β's biological effects on hepatocytes and effects on the pathogenesis of hepatocellular carcinoma caused by HCV. Furthermore, the findings of the present study may contribute to an understanding of the mechanisms underlying the TLR3 activation involved in innate immunity against viral infection. In addition, our findings suggest that an antiviral state in uninfected cells may be induced by the expression of a viral protein, NS5B.

Materials and methods

Cell culture and cell cycle analysis

The non-neoplastic immortalized human hepatocyte cell lines, PH5CH8 and NKNT-3 cells, were maintained as described previously (Ikeda et al., 1998, Kobayashi et al., 2000). Human hepatoma cell line HuH-7 cells, human cervical carcinoma HeLa cells, and HEK 293 cells were cultured in Dulbecco's modified Eagle's medium supplemented with 10% fetal bovine serum.

To synchronize the cells at the G1/S transition, growing cells were treated with thymidine (Sigma, St. Louis, MO) (2.5 mM) for 19 h, washed in PBS, and released into fresh medium for 11 h. The cells were then treated with aphidicolin (Sigma) (5 μM) for 13 h, washed in PBS, and released into fresh

medium. The cells were pulse-labeled with 10 μM bromo-deoxyuridine (BrdUrd; Sigma) for 1 h, fixed with 70% ethanol at indicated time points, stained with fluorescein-isothiocyanate (FITC)-conjugated mouse monoclonal antibody to BrdUrd (BD Pharmingen, San Diego, CA), and counterstained with propidium iodide (PI) (Sigma). The cellular content of DNA was determined by flow cytometry with FACScalibur instrument, and data were analyzed with CELL Quest software (BD Biosciences, San Jose, CA) (Naka et al., 2004). To determine the population of G2-M phase reached cells, the cells were treated with Nocodazole (Noc; Sigma) (200 ng/ml) at 5 h after release into the S phase. Then, after 7 h (post release from 12 h), the cell population that had accumulated in the G2-M phase was analyzed by flow cytometry. To examine the effects of IFN-β, PH5CH8 and NKNT-3 cells were treated with or without IFN-β (500 IU/ml) at 12 h prior to release, and cell cycle progression was analyzed. To assess the effect of anti-IFN-β neutralizing antibody, NS5B-expressing cells were treated with anti-IFN-β antibody (70 U/ml, OBT0377, Oxford Biotechnology, Oxfordshire, UK) during cell cycle synchronization and after release from the G1/S boundary.

Vector construction and retrovirus infection

Retroviral vectors pCXbsr (Akagi et al., 2000) and pCX4bsr (Akagi et al., 2003), which contain the resistance gene for blasticidin, were used in this study. The DNA fragments encoding the influenza hemagglutinin tagged (HA)-core, NS3, HA-NS4B, HA-NS5A, HA-NS5B, and NS5B were amplified from pMILE (HCV 1B-1 strain belonging to genotype 1b; accession no. AB080299) by PCR using KOD-plus DNA polymerase (Toyobo, Osaka, Japan). The obtained DNA fragments were subcloned into the EcoRI (BamHI for NS5B) and NotI sites of pCXbsr or pCX4bsr. The DNA fragment encoding myc-tagged NS5A was also amplified from pMILE by PCR. The obtained DNA fragment was subcloned into the EcoRI and NotI sites of pCXpur (Akagi et al., 2000), which contains the resistance gene for puromycin. The DNA fragments encoding TLR3 (accession no. NM_003265), Toll-IL-1 receptor (TIR) domain-containing adaptor-inducing IFN-β (TRIF or TICAM-1, accession no. NM_182919), and RIG-IC, a dominant negative inhibitor of retinoic acid-inducible gene-I (RIG-I) (Yoneyama et al., 2004), were amplified from cDNAs obtained from PH5CH8 cells. The primer sequences containing the SphI (for forward) or NotI (for reverse) recognition sites for TLR3, TRIF, and RIG-IC were designed to enable expression of the TLR3, TRIF, and RIG-IC open-reading frames, respectively. The obtained DNA fragments were subcloned into the SphI and NotI sites of pCXpur/myc, which can express myc-tagged protein. The IFN-β gene promoter region (−125 to +19) described previously (F

·8) was amplified using genomic DNA derived from PH5CH8 cells and a primer set of 5′-ACGG<u>GGTACC</u>-GAGTTTTAGAAACTACTAAAATG-3′ containing the KpnI recognition site (underlined) and 5′-AGGA<u>AGATCTTC</u>-GAAAGGTTGCAGTTAGAATG-3′ containing the BglII recognition site (underlined). The obtained DNA fragment was

subcloned into the KpnI and BglII sites of pGL3-Basic (Promega) and was termed pIFN-β(-125)-Luc. Retrovirus infections were performed as described previously (Naganuma et al., 2004).

RT-PCR and RNA interference

RT-PCR was carried out as described previously (Dansako et al., 2003). The sequences of sense and antisense primers for IFN-β (accession no. V00547) were 5'-CCCTGAGGAGATTAAG-CAGCTGC-3' and 5'-AGTTCCTTAGGATTTCCACTCTG-AC-3'. The sequences of primer set for ISG56 (accession no. X03557) were 5'-AGAAGCAGGCAATCACAGAAAAGC-TG-3' and 5'-CCAGGGCTTCATTCATATTTCCTTCC-3'. Small-interference RNA (siRNA) duplexes targeting the coding regions of human TLR3, TLR4, and luciferase GL2 (Elbashir et al., 2001) as a control were chemically synthesized (Greiner, Tokyo, Japan). The sequences of the human TLR3 oligonucleotides were: 5'-CCUCCAGCACAAUGAGCUATT-3' and 5'-UAGCUCAUUGUGCUGGAGGTT-3'. The sequences of the human TLR4 oligonucleotides were: 5'-CCUCCCCUUCUC-AACCAAGTT-3' and 5'-CUUGGUUGAGAAGGGGAGGTT-3'. The cells were transfected with the indicated siRNA duplex using OligofectAMINE (Invitrogen, Carlsbad, CA). Total RNAs were extracted after 3 days, and RT-PCR was performed using primer sets for TLR3 (Kadowaki et al., 2001), TLR4 (Kadowaki et al., 2001), and GAPDH (Dansako et al., 2003).

Western blot analysis

The preparation of cell lysates, SDS-PAGE, and immunoblotting analysis were performed according to standard procedures using primary antibodies, rat monoclonal anti-HA (3F10; Roche Molecular Biochemicals, Mannheim, Germany), mouse monoclonal anti-NS3 (clone MMM33; Novacastra Laboratories, Newcastle upon Tyne, UK), anti-NS5B (a gift from Dr. M. Kohara), anti-myc (PL14; Medical and biological laboratories, Nagoya, Japan), anti-β-actin (AC-15, Sigma), anti-STAT1 (clone 42; BD Transduction Laboratories, San Diego, CA), rabbit polyclonal anti-phospho-STAT1(Y701) (Cell Signaling Technology, Beverly, MA), and anti-IRF7 (H-246, Santa Cruz Biotechnology, Santa Cruz, CA), and horseradish-peroxidase-conjugated secondary antibodies. The immune complex was visualized using the ECL Western blot detection system (Amersham Bioscience, Piscataway, NJ).

Reporter assay

The luciferase activity was measured by dual-luciferase assay system (Promega, Madison, WI) as previously described (Dansako et al. 2003). Briefly, cells were transfected with pISRE-Luc (Stratagene, LaJolla, CA) or pIFN-β(-125)-Luc reporter plasmid together with phRL-CMV (Promega) as an internal control reporter plasmid by FuGENE6 (Roche). After 48 h of transfection, cell lysates were then prepared and assayed for luciferase activities; transfection efficiency was normalized by renilla luciferase activity (internal control) derived from phRL-CMV. Three independent triplicate transfection experiments were conducted in order to verify the reproducibly of the results.

Immunoprecipitation

Cells were lysed in a buffer containing 50 mM Tris (pH 7.4), 125 mM NaCl, 0.1%(v/v) Nonidet P-40 (NP-40; Sigma), 5 mM EDTA, 0.1 M NaF, and a mixture of protease inhibitors (Complete; Roche). Pre-cleared cell lysates were subjected to immunoprecipitation using agarose-conjugated anti-myc antibody (PL14, MBL). Bound proteins were eluted from beads by boiling in SDS sample buffer, and immunoblotting analysis was performed using anti-myc or anti-NS5B antibody, and HRP-conjugated anti-mouse IgG TrueBlot (eBioscience, San Diego, CA).

Immunofluorescence analysis

To examine the intracellular protein localization, 2×10^4 cells were cultured and treated on chamber slides then fixed and probed with polyclonal rabbit anti-IRF3 antibody (FL-425, Santa Cruz Biotechnology) and FITC-conjugated donkey anti-rabbit secondary antibody according to a method described previously (Foy et al., 2003). PH5CH8 cells treated with poly (IC) (2.5 μg/ml for 6 h; Amersham Biosciences) were used as a positive control for the activation of IRF3.

Evaluation of sensitivity to DNA damage

Cells in an exponential growth phase were plated onto 10-cm plates (5×10^3 cells/plate) and cultured for 4 days. The cells were treated with hydrogen peroxide (H_2O_2; Wako Pure Chemical, Osaka, Japan), methylmethane sulfonate (MMS; Sigma), Adriamycin (ADR; doxorubicin; Sigma), and neocarzinostatin chromophore (NCS; generously provided by Kayaku, Tokyo, Japan) for 2 h at 37 °C. For UV-B treatment (UV-B radiation at 302 nm), the medium was aspirated prior to exposure, the cells were washed twice with PBS, and then a fresh culture medium was added. Ten days later, the cells were fixed and stained with Coomassie brilliant blue as described previously (Naganuma et al., 2004). Only colonies containing >50 cells were scored as being derived from viable clonogenic cells.

Acknowledgments

References

Akagi, T., Shishido, T., Murata, K., Hanafusa, H., 2000. v-Crk activates the phosphoinositide 3-kinase/AKT pathway in transformation. Proc. Natl. Acad. Sci. U.S.A. 97, 7290–7295.

Akagi, T., Sasai, K., Hanafusa, H., 2003. Refractory nature of normal human diploid fibroblasts with respect to oncogene-mediated transformation. Proc. Natl. Acad. Sci. U.S.A. 100, 13567–13572.

Alexopoulou, L., Holt, A.C., Medzhitov, R., Flavell, R.A., 2001. Recognition of double-stranded RNA and activation of NF-kappaB by Toll-like receptor 3. Nature 413, 732–738.

Arima, N., Kao, C.Y., Licht, T., Padmanabhan, R., Sasaguri, Y., 2001. Modulation of cell growth by the hepatitis C virus nonstructural protein NS5A. J. Biol. Chem. 276, 12675–12684.

Bartenschlager, R., Lohmann, V., 2000. Replication of hepatitis C virus. J. Gen. Virol. 81, 1631–1648.

Behrens, S.E., Tomei, L., De Francesco, R., 1996. Identification and properties of the RNA-dependent RNA polymerase of hepatitis C virus. EMBO J. 15, 12–22.

Blight, K.J., Kolykhalov, A.A., Rice, C.M., 2000. Efficient initiation of HCV RNA replication in cell culture. Science 290, 1972–1974.

Bressanelli, S., Tomei, L., Rey, F.A., De Francesco, R., 2002. Structural analysis of the hepatitis C virus RNA polymerase in complex with ribonucleotides. J. Virol. 76, 3482–3492.

Colombo, M., 1996. The natural history of hepatitis C. Bailliere's Clin. Gastroenterol. 10, 275–288.

Dansako, H., Naganuma, A., Nakamura, T., Ikeda, F., Nozaki, A., Kato, N., 2003. Differential activation of interferon-inducible genes by hepatitis C virus core protein mediated by the interferon stimulated response element. Virus Res. 97, 17–30.

Dansako, H., Naka, K., Ikeda, M., Kato, N., 2005. Hepatitis C virus proteins exhibit conflicting effects on the interferon system in human hepatocyte cells. Biochem. Biophys. Res. Commun. 336, 458–469.

Dore, M.P., Realdi, G., Mura, D., Onida, A., Massarelli, G., Dettori, G., Graham, D.Y., Sepulveda, A.R., 2001 Genomic instability in chronic viral hepatitis and hepatocellular carcinoma. Hum. Pathol. 32, 698–703.

Dubourdeau, M., Miyamura, T., Matsuura, Y., Alric, L., Pipy, B., Rousseau, D., 2002. Infection of HepG2 cells with recombinant adenovirus encoding the HCV core protein induces p21(WAF1) down-regulation—Effect of transforming growth factor beta. J. Hepatol. 37, 486–492.

Elbashir, S.M., Harborth, J., Lendeckel, W., Yalcin, A., Weber, K., Tuschl, T., 2001. Duplexes of 21-nucleotide RNAs mediate RNA interference in cultured mammalian cells. Nature 411, 494–498.

Foy, E., Li, K., Wang, C., Sumpter Jr., R., Ikeda, M., Lemon, S.M., Gale Jr., M., 2003. Regulation of interferon regulatory factor-3 by the hepatitis C virus serine protease. Science 300, 1145–1148.

Foy, E., Li, K., Sumpter Jr., R., Loo, Y.M., Johnson, C.L., Wang, C., Fish, P.M., Yoneyama, M., Fujita, T., Lemon, S.M., Gale Jr., R., 2005. Control of antiviral defenses through hepatitis C virus disruption of retinoic acid-inducible gene-1 signaling. Proc. Natl. Acad. Sci. U.S.A. 102, 2986–2991.

Fujita, T., Sakakibara, J., Sudo, Y., Miyamoto, M., Kimura, Y., Taniguchi, T., 1988. Evidence for a nuclear factor(s), IRF-1, mediating induction and silencing properties to human IFN-beta gene regulatory elements. EMBO J. 7, 3397–3405.

Hagedorn, C.H., van Beers, E.H., De Staercke, C., 2000. Hepatitis C virus RNA-dependent RNA polymerase (NS5B polymerase). Curr. Top. Microbiol. Immunol. 242, 225–260.

Hsu, I.C., Tokiwa, T., Bennett, W., Metcalf, R.A. Welsh, J.A., Sun, T., Harris, C.C., 1993. p53 gene mutation and integrated hepatitis B viral DNA sequences in human liver cancer cell lines. Carcinogenesis 14, 987–992.

Ikeda, M., Sugiyama, K., Mizutani, T., Tanaka, T., Tanaka, K., Sekihara, H., Shimotohno, K., Kato, N., 1998. Human hepatocyte clonal cell lines that support persistent replication of hepatitis C virus. Virus Res. 56, 157–167.

Ikeda, M., Yi, M., Li, K., Lemon, S.M., 2002. Selectable subgenomic and genome-length dicistronic RNAs derived from an infectious molecular clone of the HCV-N strain of hepatitis C virus replicate efficiently in cultured Huh7 cells. J. Virol. 76, 2997–3006.

Jung, E.Y., Lee, M.N., Yang, H.Y., Yu, D., Jang, K.L., 2001. The repressive activity of hepatitis C virus core protein on the transcription of p21(waf1) is regulated by protein kinase A-mediated phosphorylation. Virus Res. 79, 109–115.

Kadowaki, N., Ho, S., Antonenko, S., Malefyt, R.W., Kastelein, R.A., Bazan, F., Liu, Y.J., 2001. Subsets of human dendritic cell precursors express different toll-like receptors and respond to different microbial antigens. J. Exp. Med. 194, 863–869.

Kato, N., 2001. Molecular virology of hepatitis C virus. Acta Med. Okayama 55, 133–159.

Kato, N., Hijikata, M., Ootsuyama, Y., Nakagawa, M., Ohkoshi, S., Sugimura, T., Shimotohno, K., 1990. Molecular cloning of the human hepatitis C virus genome from Japanese patients with non-A, non-B hepatitis. Proc. Natl. Acad. Sci. U.S.A. 87, 9524–9528.

Katze, M.G., He, Y., Gale Jr., M., 2002. Viruses and interferon: a fight for supremacy. Nat. Rev., Immunol. 2, 675–687.

Kobayashi, N., Fujiwara, T., Westerman, K.A., Inoue, Y., Sakaguchi, M., Noguchi, H., Miyazaki, M., Cai, J., Tanaka, N., Fox, I.J., Leboulch, P., 2000. Prevention of acute liver failure in rats with reversibly immortalized human hepatocytes. Science 287, 1258–1262.

Kondo, Y., Kanai, Y., Sakamoto, M., Mizokami, M., Ueda, R., Hirohashi, S., 2000. Genetic instability and aberrant DNA methylation in chronic hepatitis and cirrhosis-A comprehensive study of loss of heterozygosity and microsatellite instability at 39 loci and DNA hypermethylation on 8 CpG islands in microdissected specimens from patients with hepatocellular carcinoma. Hepatology 32, 970–979.

Lanford, R.E., Guerra, B., Lee, H., Averett, D.R., Pfeiffer, B., Chavez, D., Notvall, L., Bigger, C., 2003. Antiviral effect and virus–host interactions in response to alpha interferon, gamma interferon, poly(i)–poly(c), tumor necrosis factor alpha, and ribavirin in hepatitis C virus subgenomic replicons. J. Virol. 77, 1092–1104.

Leveque, V.J., Johnson, R.B., Parsons, S., Ren, J., Xie, C., Zhang, F., Wang, Q.M., 2003. Identification of a C-terminal regulatory motif in hepatitis C virus RNA-dependent RNA polymerase: structural and biochemical analysis. J. Virol. 77, 9020–9028.

Li, K., Chen, Z., Kato, N., Gale Jr., M., Lemon, S.M., 2005a. Distinct poly(I–C) and virus-activated signaling pathways leading to interferon-β production in hepatocytes. J. Biol. Chem. 280, 16739–16747.

Li, K., Foy, E., Ferreon, J.C., Nakamura, M., Ferreon, A.C.M., Ikeda, M., Ray, S.C., Gale Jr., M., Lemon, S.M., 2005b. Immune evasion by hepatitis C virus NS3/4A protease-mediated cleavage of the Toll-like receptor-3 adaptor protein, TRIF. Proc. Natl. Acad. Sci. U.S.A. 102, 2992–2997.

Lohmann, V., Korner, F., Koch, J., Herian, U., Theilmann, L., Bartenschlager, R., 1999. Replication of subgenomic hepatitis C virus RNAs in a hepatoma cell line. Science 285, 110–113.

Lu, W., Lo, S.Y., Chen, M., Wu, K., Fung, Y.K., Ou, J.H., 1999. Activation of p53 tumor suppressor by hepatitis C virus core protein. Virology 264, 134–141

Marusawa, H., Hijikata, M., Chiba, T., Shimotohno, K., 1999. Hepatitis C virus core protein inhibits Fas- and tumor necrosis factor alpha-mediated apoptosis via NF-kappaB activation. J. Virol. 73, 4713–4720.

Matsumoto, M., Kikkawa, S., Kohase, M., Miyake, K., Seya, T., 2002. Establishment of a monoclonal antibody against human Toll-like receptor 3 that blocks double-stranded RNA-mediated signaling. Biochem. Biophys. Res. Commun. 293, 1364–1369.

Medzhitov, R., 2001 Toll-like receptors and innate immunity. Nat. Rev. Immunol. 1, 135–145.

Naganuma, A., Nozaki, A., Tanaka, T., Sugiyama, K., Takagi, H., Mori, M., Shimotohno, K., Kato, N., 2000. Activation of the interferon-inducible 2'-5'-oligoadenylate synthetase gene by hepatitis C virus core protein. J. Virol. 74, 8744–8750.

Naganuma, A., Dansako, H., Nakamura, T., Nozaki, A., Kato, N., 2004. Disturbance of the DNA repair system by HCV core protein. Cancer Res. 64, 1307–1314.

Naka, K., Tachibana, A., Ikeda, K., Motoyama, N., 2004. Stress-induced premature senescence in hTERT-expressing ataxia telangiectasia fibroblasts. J. Biol. Chem. 279, 2030–2037.

Noguchi, M., Hirohashi, S., 1996. Cell lines from non-neoplastic liver and hepatocellular carcinoma tissue from a single patient. In Vitro Cell. Dev. Biol. 32, 135–137.

Oshiumi, H., Matsumoto, M., Funami, K., Akazawa, T., Seya, T., 2003. TICAM-1, an adaptor molecule that participates in Toll-like receptor 3-mediated interferon-beta induction. Nat. Immunol. 4, 161–167.

Ray, R.B., Ray, R., 2001. Hepatitis C virus core protein: intriguing properties and functional relevance. FEMS Microbiol. Lett. 202, 149–156.

Ray, R.B., Steele, R., Meyer, K., Ray, R., 1998. Hepatitis C virus core protein represses p21WAF1/Cip1/Sid1 promoter activity. Gene 208, 331–336.

Reed, K.E., Rice, C.M., 2000. Overview of hepatitis C virus genome structure, polyprotein processing, and protein properties. Curr. Top. Microbiol. Immunol. 242, 55–84.

Schmidt-Mende, J., Bieck, E., Hugle, T., Penin, F., Rice, C.M., Blum, H.E., Moradpour, D., 2001. Determinants for membrane association of the hepatitis C virus RNA-dependent RNA polymerase. J. Biol. Chem. 276, 44052–44063.

Scholle, F., Li, K., Bodola, F., Ikeda, M., Luxon, B.A., Lemon, S.M., 2004. Virus–host cell interactions during hepatitis C virus RNA replication: impact of polyprotein expression on the cellular transcriptome and cell cycle association with viral RNA synthesis. J. Virol. 78, 1513–1524.

Shi, S.T., Lee, K.J., Aizaki, H., Hwang, S.B., Lai, M.M., 2003. Hepatitis C virus RNA replication occurs on a detergent-resistant membrane that cofractionates with caveolin-2. J. Virol. 77, 4160–4168.

Shirota, Y., Luo, H., Qin, W., Kaneko, S., Yamashita, T., Kobayashi, K., Murakami, S., 2002. Hepatitis C virus (HCV) NS5A binds RNA-dependent RNA polymerase (RdRP) NS5B and modulates RNA-dependent RNA polymerase activity. J. Biol. Chem. 277, 11149–11155.

Takeda, K., Kaisho, T., Akira, S., 2003. Toll-like receptors. Annu. Rev. Immunol. 21, 335–376.

Thomas, D.L., 2000. Hepatitis C epidemiology. Curr. Top. Microbiol. Immunol. 242, 25–41.

Tsuchihara, K., Hijikata, M., Fukuda, K., Kuroki, T., Yamamoto, N., Shimotohno, K., 1999. Hepatitis C virus core protein regulates cell growth and signal transduction pathway transmitting growth stimuli. Virology 258, 100–107.

Vannucchi, S., Percario, Z.A., Chiantore, M.V., Matarrese, P., Chelbi-Alix, M.K., Fagioli, M., Pelicci, P.G., Malorni, W., Fiorucci, G., Romeo, G., Affabris, E., 2000. Interferon-beta induces S phase slowing via up-regulated expression of PML in squamous carcinoma cells. Oncogene 19, 5041–5053.

Wakita, T., Pietschmann, T., Kato, T., Date, T., Miyamoto, M., Zhao, Z., Murthy, K., habermann, A., Krausslich, H.G., Mizokami, M., Bartenschlager, R., Liang, T.J., 2005. Production of infectious hepatitis C virus in tissue culture from a cloned viral genome. Nat. Med. 11, 791–796.

Yamamoto, M., Sato, S., Mori, K., Hoshino, K., Takeuchi, O., Takeda, K., Akira, S., 2002. Cutting edge: a novel Toll/IL-1 receptor domain-containing adapter that preferentially activates the IFN-beta promoter in the Toll-like receptor signaling. J. Immunol. 169, 6668–6672.

Yamamoto, M., Sato, S., Hemmi, H., Hoshino, K., Kaisho, T., Sanjo, H., Takeuchi, O., Sugiyama, M., Okabe, M., Takeda, K., Akira, S., 2003. Role of adaptor TRIF in the MyD88-independent toll-like receptor signaling pathway. Science 301, 640–643.

Yamashita, T., Kaneko, S., Shirota, Y., Qin, W., Nomura, T., Kobayashi, K., Murakami, S., 1998. RNA-dependent RNA polymerase activity of the soluble recombinant hepatitis C virus NS5B protein truncated at the C-terminal region. J. Biol. Chem. 273, 15479–15486.

Yoneyama, M., Kikuchi, M., Natsukawa, T., Shinobu, N., Imaizumi, T., Miyagishi, M., Taira, K., Akira, S., Fujita, T., 2004. The RNA helicase RIG-I has an essential function in double-stranded RNA-induced innate antiviral responses. Nat. Immunol. 5, 730–737.

Zhu, Q., Guo, J.T., Seeger, C., 2003. Replication of hepatitis C virus subgenomes in nonhepatic epithelial and mouse hepatoma cells. J. Virol. 77, 9204–9210.

＜特集関連情報＞

献血者における HBV 陽性率の動向と B 型肝炎感染初期例の HBV 遺伝子型頻度

　わが国の輸血用血液は1960年代半ばまでそのほとんどが売血によりまかなわれていた。その売血時代には輸血を受けた患者の約半数が輸血後肝炎を発症していたと報告されているが，その後の献血制度への切り替え，新たな検査の導入や献血前の問診の強化などにより輸血用血液の安全性は飛躍的に高まっていった。特に B 型肝炎ウイルス（HBV），C 型肝炎ウイルス（HCV），ヒト免疫不全ウイルス（HIV）に対する核酸増幅検査（NAT）が導入された1999年以降は，輸血によるこれらのウイルス感染の報告は大きく減少した。このようにして現在，わが国の輸血用血液の安全性は世界のトップレベルとなっている。本稿ではかつて「日本の国民病」とまでいわれた B 型肝炎に的を絞り，輸血用血液スクリーニング検査における HBV 陽性率の推移と，HBV-NAT で見出された感染初期例の HBV 遺伝子型の出現頻度の変動について述べ，HBV 感染の現状を考察したい。

　HBs 抗原検査は1972年に導入され当初は免疫電気泳動法により行われていたが，1978年に血球凝集法に変更された。また輸血用血液のさらなる安全性向上のため1989年末には HBc 抗体検査を新たに導入した。表1に1985年～2005年までの全国の HBs 抗原陽性率と HBc 抗体陽性率を示す。HBs 抗原陽性率は1988年以降ほぼ直線的に減少し，2005年には0.05％にまで低下している。HBs 抗原検査で陽性となった献血者へは医療機関への受診を勧めるとともに，安全な血液供給のために以降の献血を辞退していただく旨の通知をしている。一方，HBc 抗体陽性率は幾度かの陽性基準変更後，2003年4月から通知を開始している。

　B 型肝炎の撲滅を目指して，1985年から一部の医療機関で，1986年からは全国の医療機関で「B 型肝炎ウイルスの母子感染防止対策事業」が開始された。この事業の効果を確認するため1995年から茨城県，栃木県，東京都，神奈川県および福岡県の1都4県で，16歳初回献血者の HBs 抗原陽性率の調査を継続している。初回献血者は通知による選択を受けないため，その陽性率は地域住民の陽性率を反映すると考えられている。上記の地域における16歳初回献血者の HBs 抗原陽性率は，1995年から直線的に低下し，2003年にはゼロとなった（図1）。2004年には若干の陽性例が認められたが，この年の陽性者はすべて水平感染であることが確認されており，2003年～2005年までの3年間に16歳初回献血者で HBV キャリアは確認されていない。2002年の16歳はすべて事業開始後に出生した児であるが，陽性例はキャリアであるか否かの確認が取れていない。以上，限られた地域ではあるが「B 型肝炎ウイルスの母子感染防止対策事業」の効果が改めて確認されている。

　日本における HBV キャリアは遺伝子型 C が最も多く85％を占め，次いで遺伝子型 B が12％，欧米型の遺伝子型 A および D はそれぞれ1.7％，0.4％で，その他の遺伝子型は検出されなかったと報告されている。一方，最近の急性 B 型肝炎例の HBV 遺伝子型出現頻度は，キャリア例と大きく異なることが医療機関から報告されている。NAT スクリーニングは血清学的検査陰性検体のみを対象として行っているため，NAT で検出される例はほとんどが感染初期例である。これらの例から HBc 抗体陽性のキャリアを排除し，感染初期例のみの HBV 遺伝子型出現頻度を調べると，NAT

表1. HBVスクリーニング検査陽性率

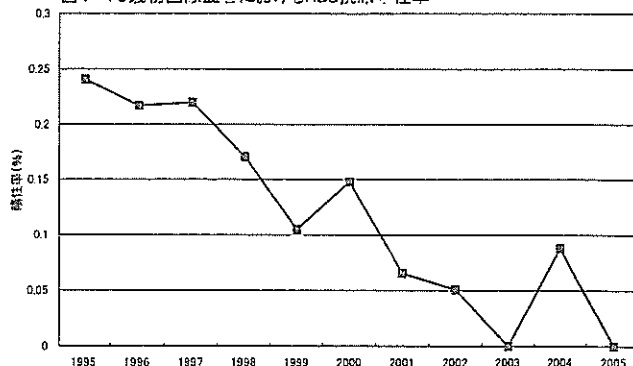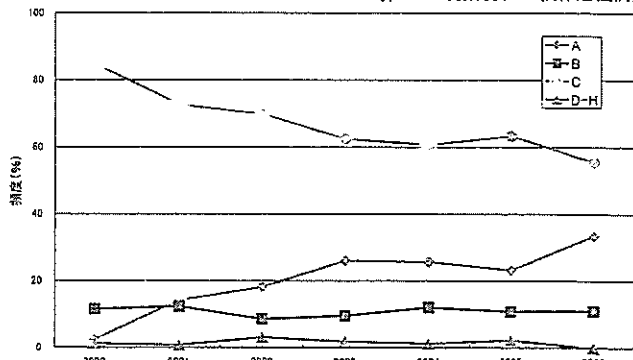| 年	陽性率(%)	
	HBs抗原	HBc抗体
1985	1.28	—
1986	1.28	—
1987	1.29	—
1988	1.05	—
1989	0.95	—
1990	0.80	1.09
1991	0.64	1.00
1992	0.51	0.95
1993	0.41	1.12
1994	0.34	1.60
1995	0.31	1.64
1996	0.25	1.62
1997	0.21	2.00
1998	0.17	2.20
1999	0.15	2.01
2000	0.13	1.85
2001	0.12	1.57
2002	0.10	1.32
2003	0.09	1.21
2004	0.07	0.66
2005	0.05	0.45

図1　16歳初回献血者におけるHBs抗原陽性率

図2. HBV−NAT で見出されたHBV Genotypeの出現頻度（HBc抗体陰性例）

導入直後の2000年の出現頻度はキャリア例の頻度とほぼ同等であった（前ページ図2）。しかし，その後は遺伝子型Aの頻度が年々増加し，その分だけ遺伝子型Cが減少していた。急性B型肝炎の感染経路はほとんどが性的接触によるといわれている。また遺伝子型Aは免疫抑制状態でない成人への感染でも約10％がキャリア化するといわれており，欧米型HBVが日本に根付きつつあることが推測される。NATスクリーニングで検出された遺伝子型Aのほぼ全例が男性であるのも興味深い。

<div align="right">東京都西赤十字血液センター　内田茂治</div>

＜速報＞

麻しんの地域流行——千葉市

2006年4月より茨城県から千葉県にかけて麻しんが流行し，継続的な患者発生が確認されている。千葉市内においても小学校，高校，および大学での集団感染が認められ，小学校の集団事例，および散発事例から合計7株の麻疹ウイルスを検出したのでその概要について報告する。

本年4月上旬，市内の学校から麻しんの集団感染が認められる旨の情報提供が千葉市保健所にあった。保健所が管内における発生状況等を調査したところ，A大学，B高校，C高校，およびD小学校において集団感染が確認された。患者発生は，A大学で4月上旬〜5月上旬，B高校で5月上旬〜6月中旬，C高校で6月上旬〜6月下旬，およびD小学校で5月上旬〜7月中旬まで継続した。各学校の患者数，およびワクチン接種状況を表1に示した。なお，本年7月14日現在で市内の麻しん患者数は集団感染事例と散発事例を合わせて144名となった。

表1　麻しん患者数（2006年7月14日現在）

学校	在籍者数	麻しん患者		
		患者数	ワクチン接種または罹患歴あり	未接種者数
A大学	1120	11	1	10
B高校	346	43	31	12
C高校	114	13	12	1
D小学校	332	21	18	3

このような状況から当所では，5月〜6月にかけて市内医療機関において採取された患者の咽頭ぬぐい液7検体（D小学校の集団感染例4名，および散発例3名）についてB95a細胞によるウイルス分離とRT-PCRを実施したところ，分離培養では2検体から麻疹ウイルスが分離され，RT-PCRでは7検体すべてから麻疹ウイルス遺伝子が検出されたが，そのうちの5検体が2006年以前の麻しんワクチン接種者であった（表2）。

ダイレクトシークエンスによりPCR産物の塩基配列（N遺伝子3'末端領域456bp）を決定し，そのうちの385bp（position: 1301-1685）についてNJ法による分子系統樹解析を行った。その結果，D小学校の集団感染例4株は日本固有の遺伝子型D5に分類（Bangkok. THA/93/1と同一のクラスター）され，その配列はすべて一致した。一方，散発例3株は中国と韓国に固有の遺伝子型H1に分類（Hunan.CHN/93/7と同一のクラスター）され，その配列もすべて一致した。また，N遺伝子3'末端領域（456bp）を用いたBLAST2 searchの結果，遺伝子型D5に分類された株はMVi/Queensland. AU/37.03と100％の相同性を有し，遺伝子型H1に分類された株はMVs/Taipei.TWN/11.93と100％の相同性，国内で分離されている株ではMVi/Tokyo.JPN/20.00(S)と最も高い相同性（99.0％）を有していた。

千葉市で検出された麻疹ウイルスの遺伝子型は，2001年がD5型，2002年と2003年はH1型が主流行株であった。本年は集団感染例からD5型，散発事例からH1型が検出されているが，今後もウイルス分離を含めた野外麻疹ウイルス株の遺伝子型の解析は公衆衛生学上重要であることから，その動向に注目したい。なお，散発例から検出された麻疹ウイルスH1型の3株のうち1株（症例5）は明らかに中国（北京）滞在中に感染したものであり，他の2株（症例6と7）は海外渡航歴がなく国内での感染であったが，これら3株の配列（N遺伝子3'末端領域456bp）が同一であったことから，現在もなお中国や韓国の流行株であるH1型が日本に持ち込まれ，伝播している可能性が強く示唆された。

今回の地域流行によって，大学，高校，および小学校の年代に感受性者が多数存在することが推測されたものの，市内の感染症発生動向調査定点から最初に患者数が報告されたのは，第20週（定点当たり患者数0.06人）であった。その後，定点当たり患者数は0.06人〜0.13人の間で推移し，明らかな集団発生は確認されて

表2. 麻疹ウイルスの検出症例および検査結果

症例	年齢	性別	検体	臨床症状	発病日	採取日	分離	PCR	遺伝子型	ワクチン接種	発生状況等
1	6歳3カ月	男	咽頭ぬぐい液	発熱（38.5℃）、上気道炎、発疹	5月16日	5月19日	+	+	D5	有（2001/2/28）	集団発生（小学校）
2	6歳7カ月	女	咽頭ぬぐい液	発熱（39.0℃）、気管支炎、発疹、Koplik斑	5月19日	5月22日	−	+	D5	有（2001/2/8）	集団発生（小学校）
3	6歳5カ月	女	咽頭ぬぐい液	発熱（39.6℃）、発疹、リンパ節腫脹、Koplik斑	5月17日	5月22日	−	+	D5	有	集団発生（小学校）
4	7歳2カ月	女	咽頭ぬぐい液	発熱（39.3℃）、上気道炎、発疹、リンパ節腫脹	5月20日	5月23日	+	+	D5	有（2000/10/26）	集団発生（小学校）
5	1歳0カ月	男	咽頭ぬぐい液	発熱（39.0℃）、発疹	5月14日	5月19日	−	+	H1	なし	中国（北京）滞在中に発症
6	2歳8カ月	女	咽頭ぬぐい液	発熱（39.0℃）、発疹	5月6日	5月8日	−	+	H1	有（2004/12/27）	散発例
7	1歳	男	咽頭ぬぐい液	発熱（40.0℃）、発疹	6月1日	6月6日	−	+	H1	有（2006/6/1）	散発例

Neutralization of HPV16, 18, 31, and 58 pseudovirions with antisera induced by immunizing rabbits with synthetic peptides representing segments of the HPV16 minor capsid protein L2 surface region

Kazunari Kondo [a,b], Yoshiyuki Ishii [a], Hiroyuki Ochi [a,b], Tamae Matsumoto [a], Hiroyuki Yoshikawa [b], Tadahito Kanda [a,*]

[a] Center for Pathogen Genomics, National Institute of Infectious Diseases, 1-23-1 Toyama, Shinjuku-ku, Tokyo 162-8640, Japan
[b] Department of Obstetrics and Gynecology, University of Tsukuba, 1-1-1 Tennoudai, Tsukuba-shi, Ibaraki 305-8575, Japan

Abstract

Neutralizing antibody against human papillomavirus (HPV) minor capsid protein L2 can cross-neutralize different HPV genotypes in vitro. To identify the segments containing the cross-neutralization epitopes of HPV16 L2, we characterized antisera obtained by immunizing two rabbits with each of the ten synthetic peptides of 14 to 20 amino acids (aa) long, which represents a part of the HPV16 L2 sequence from aa 14 to 144. The antisera against the peptides within the region from aa 18 to 144 efficiently bound to HPV16 L1/L2-capsids and neutralized HPV16 pseudovirions, indicating that the region is displayed on the surface of the capsids and contains several neutralization epitopes. Antiserum against the peptide from aa 18 to 38 (anti-P18/38) cross-neutralized HPV18. Anti-P56/75 cross-neutralized HPV18, 31, and 58. Anti-P61/75 and anti-P64/81 cross-neutralized HPV18 and 58. Anti-P96/115 and the antiserum induced by a mutant P96/115 (S and T at aa 101 and 112 were replaced with L and S, respectively) cross-neutralized HPV31 and 58. The mixture of equal volumes of three antisera, anti-P18/38, anti-P56/75, and anti-mutant P96/115, neutralized HPV16, 18, 31, and 58 more efficiently than anti-P56/75 alone, suggesting that there is a synergistic effect of antibodies on the cross-neutralization. The cross-neutralization appears to be correlated with conserved aa sequences among HPV types. The data in this study provide a basis for designing vaccine antigens effective against a broader spectrum of the high-risk HPVs.
© 2006 Elsevier Inc. All rights reserved.

Keywords: HPV16; Minor capsid protein L2; Neutralization epitope

Introduction

Human papillomavirus (HPV) is a small nonenveloped virus having an 8-kb double-stranded circular DNA. To date more than 100 HPV genotypes, classified based on the homology of genomic DNA, have been identified in proliferative lesions of skin or mucosa (Stoler, 2000). HPVs that infect the genital mucosal epithelia are divided into two groups: low-risk types (such as types of 6 and 11) found mainly in benign condyloma and 15 high-risk types (types of 16, 18, 31, 33, 35, 39, 45, 51, 52, 56, 58, 59, 66, 68, and 73) (Munoz et al. 2004) found in cervical cancer, the most frequent gynecological cancer in the world (Ferlay et al. 1998; Ione 999). Although the distribution of high-risk HPVs in humans slightly varies from region to region, type 16 (HPV16) accounts for about 50% of the cases worldwide (Munoz et al., 2004).

An icosahedral HPV capsid is composed of major capsid protein L1 and minor capsid protein L2. Since it is difficult to obtain a large amount of HPV particles by using conventional cell cultures, surrogate systems capable of expressing L1 and L2 have been developed to obtain HPV capsids for structural and immunological analysis. Expression of L1 either alone or together with L2 in cultured cells results in production of L1 capsids (also called virus-like particle; VLP) (Kirnbauer et) or L1/L2-capsids ( ). The L1 capsid is composed of 360 L1 molecules arranged as 72 pentameric capsomeres (Baker et al 99 Crawford and Crawford 1963), and the L1/L2-capsid contains additional 12 L2 molecules whose N-terminal region is displayed on the surface of

* Corresponding author. Fax: +81 3 5285 1166.
E-mail address: kanda@nih.go.jp (T. Kanda).

the capsids (Heino et al., 1995; Liu et al., 1997). These particles are morphologically indistinguishable by electron microscopy from HPV virions extracted from the lesions (Kirnbauer et al., 1992).

Expression of L1 and L2 in cells harboring episomal copies of BPV1 genome or an expression plasmid results in packaging of the episomal DNA into the L1/L2-capsids to produce infectious pseudovirions (Buck et al., 2004; Roden et al., 1996; Stauffer et al., 1998; Unckell et al., 1997; Zhao et al., 1998; Zhou et al., 1993). Although it is not clear whether the pseudovirions are assembled in the same way as the authentic HPV virion, the pseudovirions are used as a surrogate virus to detect neutralizing activity of anti-HPV antibodies.

Anti-L1 antibodies obtained by immunizing mice or rabbits with the L1 capsids have been shown to have primarily type-specific neutralizing activity. Limited cross-neutralizing activity has been observed between closely related types such as HPV18 and 45, and HPV6 and HPV11 (Giroglou et al., 2001). Anti-L1 antibodies can protect animals against challenge with animal papillomaviruses (Breitburd et al., 1995; Suzich et al., 1995). The L1 capsids of HPV6, 11, 16, and 18 were used in the recent clinical trials as prophylactic vaccines, which successfully induced type-specific neutralizing antibodies in recipients (Harper et al., 2006; Villa et al., 2005).

Anti-L2 antibodies have cross-neutralizing activity in vitro. Roden et al. (2000) showed that the antisera obtained by immunizing sheep with bacterially produced L2s of HPV6, 16, and 18 neutralize the pseudovirions of homologous HPV types and cross-neutralize those of the heterologous HPV types. Kawana et al. (1999) showed that a mouse monoclonal antibody recognizing a linear epitope within HPV16 amino acids (aa) 108–120 inhibits infection with HPV16 and 6 pseudovirions, which were produced by an in vitro packaging method. Recently, Pastrana et al. (2005) reported that antibodies to bovine papillomavirus type 1 (BPV1) L2 aa 1–88 neutralize HPV16, 18, and BPV1 pseudovirions and HPV11 native virions efficiently and HPV31, 6 and cottontail rabbit papillomavirus pseudovirions less efficiently.

Vaccination of animals with L2 protects animals from animal papillomavirus challenge similarly to vaccination of animals with the L1 capsids. Embers et al. (2002) showed that immunization of rabbits with the peptides having amino acid sequences of rabbit oral (ROPV) and cutaneous (CRPV) papillomavirus L2 segments corresponding to HPV16 L2 aa 108–120 protect the rabbits from challenge with ROPV and CRPV, respectively. The level of protection induced by these peptides is comparable to that with L1 capsid vaccination. These data, together with the cross-neutralization activity of anti-L2 antibody in vitro, suggest that L2-vaccine may induce antibody protecting against a broad spectrum of the high-risk HPVs. The detailed characterization of L2-neutralization epitopes is required to design L2-vaccine antigens.

In this study we produced antisera by immunizing rabbits with synthetic peptides representing segments of the HPV16 L2 surface region and examined their neutralizing activity against HPV16 and cross-neutralizing activities against HPV18, 31, and 58.

Results and discussion

Binding of anti-L2-peptide rabbit antisera with L1/L2-capsid

We searched for potentially immunogenic segments within the N-terminal region (amino acids [aa] 1–150) of HPV16 L2 by using a computer program (Lasergene Soft ver.6, DNA Star Inc., Madison, WI). The peptides representing the aa sequences of the predicted antigenic segments and three mutant peptides (Fig. 1) were synthesized and conjugated with keyhole limpet hemocyanin (KLH). Numbering of aa in L2 of HPV 16 is deduced from the revised sequence of HPV16 (HPV16R) registered in the HPV Sequence Database (Los Alamos National Laboratory, NM). The peptide having aa sequence corresponding to HPV16 L2 aa 14 to 27 was designated as P14/27. The other peptides were designated similarly. Peptides P28/42(32V, 39T) (D at aa 32 and K at aa 39 of P28/42 were replaced with V and T, respectively), P61/75(73V) (I at aa 73 of P61/75 was replaced with V), and P96/115(101L, 112S) (S at aa 101 and T at aa 112 of P96/115 were replaced with L and S, respectively) were designed to convert the original aa into those of majority of the oncogenic HPVs. The immunization of two

P14/27	SATQLYKTCKQAGT
P18/38	LYKTCKQAGTCPPDIIPKVEG
P28/42	CPPDIIPKVEGKTIA
P28/42 32V,39T	CPPDVIPKVEGTTIA
P56/75	CGGLGIGTGSGTGGRTGYIPL
P61/75	CGTGSGTGGRTGYIPL
P61/75 73V	CGTGSGTGGRTGYVPL
P64/81	CSGTGGRTGYIPLGTRPPT
P90/111	CRPPLTVDPVGPSDPSIVSLVEE
P96/115	CDPVGPSDPSIVSLVEETSFI
P96/115 101L,112S	CDPVGPLDPSIVSLVEESSFI
P107/122	CSLVEETSFIDAGAPTS
P131/144	SGFSITTSTDTTPAC

Fig. 1 Synthetic peptides used as antigens for immunizing rabbits. The potentially immunogenic segments were searched for within the HPV16 L2 surface region. The peptides having the amino acid sequences of the predicted antigenic regions were synthesized and conjugated with keyhole limpet hemocyanin (KLH). The numbers above the amino acid sequences are amino acid number of HPV16 L2, which consists of 473 amino acids. The N-terminal Cs of P56/75, P61/75, P61/75(73V), P64/81, P90/111 P96/115, P96/115(101L, 112S), and P107/122 and the C-terminal C of P131/144 were added for the C-mediated conjugation reaction. Two rabbits were immunized with each peptide.

rabbits with each of the peptide antigens induced antibodies with binding titers of 8000 to 64,000. The binding titer was expressed as a reciprocal of the maximum dilution of serum that induced higher OD than that the corresponding preimmune serum diluted at 1 to 100 did (data not shown).

Table 1 shows the bindings of the antisera that were diluted at 1 to 500 to the L1 capsids of HPV16, the L1/L2-capsids of HPV16, 18, 31, and 58 by ELISA. The antiserum from rabbit #1 immunized with P-14/27 (anti-P14/27#1) did not react to the L1/L2-capsids, but anti-P14/27#2 reacted to the L1/L2-capsids. Because both antisera were highly reactive to P14/27, P14/27 probably contained at least two epitopes. The epitope recognized by anti-P14/27#1 appears not to be displayed on the surface of the L1/L2-capsid, suggesting that the N-terminal border between the inside and surface region of L2 is within the segment from aa 14 to 27. The other sera against the peptides having the authentic aa sequences of HPV16 L2 were found to bind to HPV16 L1/L2-capsids, indicating the L2 region from aa 18 to 144 is displayed on the surface of the L1/L2-capsids.

Anti-P56/75#1 and #2, anti-P61/75#1 and #2, anti-P64/81#1 and #2, anti-P90/111#1, anti-P96/115#1and #2 cross-bound to the L1/L2-capsids of HPV18, 31, and 58. Anti-P90/111#2 did not bind to the L1/L2-capsids of HPV18 and 58. It is possible that epitope(s) recognized by anti-P90/111#2 may be different from those recognized by anti-P90/111#1.

Although anti-P28/42 sera bound to HPV16 L1/L2-capsids efficiently and to HPV58 L1/L2-capsids less efficiently, anti-P28/42(32V, 39T) bound to HPV16 L1/L2-capsids with a low

efficiency and did not bind to the L1/L2-capsids of HPV18, 31, and 58. The result strongly suggests that D at aa 32 and K at aa 39 are associated with the epitope.

Anti-P61/75(73V)#1 and #2 and anti-P96/115(101L, 112S) #2 bound to the L1/L2-capsids of HPV16, 18, 31, and 58, suggesting that P61/75(73V) and P96/115(101L, 112S) have potential to induce antibodies capable of binding to the 15 oncogenic HPVs.

Neutralization of HPV16, 18, 31, and 58 pseudovirions with the rabbit antisera

Neutralizing activities of the antisera were measured by inhibition of infection of 293TT cells, a human fibroblast cell line expressing a high level of SV40 T-antigen, with infectious HPV16, 18, 31, and 58 pseudovirions containing the SEAP expression plasmid having the SV40 replication origin. Serum was mixed with the pseudovirion stock and then inoculated to 293TT cells. Seventy-two hours later the SEAP activity of the culture medium was measured. The neutralizing titer was expressed as a reciprocal of the maximum dilution of serum that reduced the level of SEAP activity to half of the sample not treated with serum (Table 2).

Anti-P14/27#1 and #2 did not neutralize the pseudovirions tested in agreement with the lack of their efficient binding to the L1/L2-capsids (Table 1).

Anti-P18/38 neutralized HPV16 and cross-neutralized HPV18. Although the antisera diluted at 1 to 500 did not bind to the HPV18 L1/L2-capsids efficiently (Table 1), the antisera bound to HPV18 pseudovirions (data not presented), suggesting that the capsid containing DNA may be somewhat different from the empty capsid conformationally.

Anti-P28/42#1 did not neutralize HPV16 nor cross-neutralized HPV18, 31, and 58. Anti-P28/42#2, which bound to the HPV16 L1/L2-capsids more efficiently than anti-P28/42#1 (Table 1), neutralized HPV16 and cross-neutralized HPV58. Because anti-P28/42#1 and anti-P28/42#2 showed a similar binding efficiency to the HPV58 L1/L2-capsid, antibodies in these antisera probably recognized different epitopes.

Anti-P56/75#1 and #2 neutralized HPV16 and cross-neutralized HPV18, 31, and 58. Anti-P61/75#1 and #2 and anti-P64/81#1 and #2 neutralized HPV16 and cross-neutralized HPV18 and 58. Based on the comparison of the aa sequences of P56/75, P61/75, and P64/81, we speculated that P56/75 may induced antibody recognizing the portion from aa 56 to 61, of which aa sequences are common among the 15 oncogenic HPVs (Fig. 2). Because anti-P61/75 and anti-P64/81 did not cross-neutralize HPV31 despite the efficient binding to HPV31 L1/L2-capsids (Table), it is strongly suggested that the binding is necessary but not sufficient for the neutralization.

Both anti-P90/111#1 and #2 neutralized HPV16, and anti-P90/111#2 cross-neutralized HPV31. Anti-P96/115#1 and #2 neutralized HPV16. Anti-P96/115#2, which bound to the L1/L2-capsids more efficiently than anti-P96/115#1, efficiently cross-neutralized HPV31 and HPV58 but did not HPV18. Anti-P107/122#1 and anti-P131/144#2 neutralized HPV16 exclusively.

Table 1
Binding of antibody to the L1/L2-capsids of HPV16, 18, 31 and 58 (absorbency in ELISA with serum diluted at 1 to 500)

Antiserum/Antigen		HPV16 L1	HPV16 L1/L2	HPV18 L1/L2	HPV31 L1/L2	HPV58 L1/L2
Anti-P14/27	#1	0.066	0.066	0.044	0.053	0.061
	#2	0.064	0.112	0.055	0.057	0.138
Anti-P18/38	#1	0.069	0.744	0.057	0.067	0.124
	#2	0.160	0.457	0.065	0.090	0.100
Anti-P28/42	#1	0.085	0.255	0.055	0.113	0.159
	#2	0.084	0.547	0.061	0.091	0.156
Anti-P28/42 (32V, 39T)	#1	0.093	0.106	0.058	0.075	0.053
	#2	0.089	0.135	0.059	0.070	0.070
Anti-P-56/75	#1	0.068	0.951	0.717	0.807	0.514
	#2	0.085	1.022	0.565	0.336	0.462
Anti-P61/75	#1	0.066	0.954	0.634	0.444	0.271
	#2	0.109	0.884	0.612	0.343	0.553
Anti-P61/75 (73V)	#1	0.075	0.700	0.379	0.421	0.170
	#2	0.075	0.694	0.269	0.427	0.153
Anti-P64/81	#1	0.226	1.033	0.838	0.693	0.340
	#2	0.112	1.029	0.647	0.717	0.205
Anti-P90/111	#1	0.104	1.049	0.367	0.561	0.265
	#2	0.078	0.879	0.085	0.459	0.096
Anti-P96/115	#1	0.087	0.984	0.436	0.491	0.172
	#2	0.102	1.049	0.808	0.757	0.570
Anti-P96/115 (101L, 112S)	#1	0.075	0.840	0.070	0.808	0.430
	#2	0.043	0.841	0.421	0.672	0.571
Anti-P107/122	#1	0.086	1.034	0.068	0.149	0.309
Anti-P131/144	#1	0.072	0.497	0.048	0.077	0.052
	#2	0.119	0.921	0.056	0.064	0.072

Table 2
Neutralization of HPV16, 18, 31, and 58 pseudovirions with the antisera

Antiserum		HPV16	HPV18	HPV31	HPV58
		Neutralizing titer against			
Anti-P14/27	#1	<50	<50	<50	<50
	#2	<50	<50	<50	<50
Anti-P18/38	#1	800	50	<50	<50
	#2	400	100	<50	<50
Anti-P28/42	#1	<50	<50	<50	<50
	#2	800	<50	<50	50
Anti-P28/42,	#1	<50	<50	<50	<50
32V, 39T	#2	<50	<50	<50	<50
Anti-P56/75	#1	400	200	200	400
	#2	200	50	100	200
Anti-P61/75'	#1	400	100	<50	50
	#2	800	200	<50	100
Anti-P61/75,	#1	100	<50	<50	<50
73V	#2	100	<50	50	<50
Anti-P64/81	#1	3200	400	<50	100
	#2	800	200	<50	50
Anti-P90/111	#1	200	<50	50	<50
	#2	200	<50	<50	<50
Anti-P96/115	#1	200	<50	50	<50
	#2	400	<50	400	200
Anti-P96/115,	#1	100	<50	200	200
101L, 112S	#2	100	50	100	100
Anti-P107/122	#1	100	<50	<50	50
Anti-P131/144	#1	<50	<50	<50	<50
	#2	200	<50	<50	<50

Table 3
Neutralization of HPV16, 18, 31, and 58 pseudovirions with the mixture of three antisera

Mixture of antisera	HPV16	HPV18	HPV31	HPV58
	Neutralizing titer			
Anti-P18/38 #2				
Anti-P56/75 #1	1600	800	800	400
Anti-P96/115 (101L, 112S) #1				
Anti-P18/38 #2				
Anti-P56/75 #1	800	800	400	100
Preimmune for P96/115 (10L1, 112S) #1				
Preimmune for P18/38 #2				
Anti-P56/75 #1	100	50	50	50
Preimmune for P96/115 (101L, 112S) #1				
Preimmune for P18/38 #2				
Preimmune for P56/75 #1	<50	<50	<50	<50
Preimmune for P96/115 (101L, 112S) #1				

Among antisera induced by the peptides having aa substitutions, anti-P96/115(101L, 112S) showed efficient cross-neutralization. Anti-P96/115(101L, 112S)#1 neutralized HPV16, 31, and 58. Anti-P96/115(101L, 112S)#2 neutralized the all HPVs tested.

We selected three antisera, anti-P18/38#2, anti-P56/75#1, and anti-P96/115(101L, 112S)#1, which showed the cross-neutralizing activity and the antigens used to obtain these antisera do not overlap each other, mixed equal volumes of these antisera, and

the mixture's neutralizing activity was measured similarly. The mixture neutralized HPV16, 18, 31, and 58 efficiently. When anti-P18/38#2 and anti-P96/115(101L, 112S)#1 were replaced with preimmune serum, neutralization activity was lowered. The data suggest that the bindings of multiple antibodies to the L2 surface region enhance neutralization of HPVs.

In summary, the data in this study indicate that multiple neutralization epitopes are present within the HPV16 L2 surface region, from aa 18 to 144. It was suggested that some of the peptide antigens having highly conserved aa sequences in the L2 surface region among oncogenic HPVS would have a potential to induce type common neutralization antibodies. From the data of the neutralization tests with the mixtures of three antisera (Table 3), it was suggested that the effective neutralization could be achieved through the binding of multiple antibodies to the L2 surface. It appears to be a good idea to


```
                                           56         61                                    ▼               ▼
HPV16  18-LYKTCKQAGTCPPDIIPKVEG-38  56-GGLGIGTGSGTGGRTGYIPLGTRPPT-81  96-DPVGPSDPSIVSLVEETSFI-115
HPV18  17-*******S*******VV*****-37  55-*****************************G*SN*-80  94-E****T*****T*I*DS*VV-113
HPV31  18-**Q***A*****S*V***I*H-38  56-******S***********V**S***S*-81  96-*****L**********SGIV-115
HPV58  17-**Q***AS******V*****-37  55-*****************V***ST**S-80  95-*T***L*S*****I**S***-114
HPV33  17-**Q***AT*****V******-37  55-*****************V*I**D***-80  95-*T***L*S****I******-114
HPV35  18-**R***A*****V******-38  56-******S*****S**V****T****-81  100-*TI**L*S************-119
HPV39  17-**R****S*****VVD****-37  55-******T***********G**N*-80  94-E****E***Q***DS*V*-113
HPV45  17-**R****S*****V*N****-37  55-*****S*****V***G*SN*-80  94-E****T*****T***DS*VV-113
HPV51  17-**S***A******VVN****-37  55-*****S***********GGGRP-80  95-*LWHHTE***N***DS*I*-114
HPV52  17-**Q***AS*****V*****-37  55-**A*S***A**V**S*****-80  95-E*I**LE*****MI***T**-114
HPV56  17-******LS****E*VVN*I*Q-37  55-**T*S***A**V***S**S*-80  94-ES***T*****T****S*V*-113
HPV59  17-***********S*V*N****-37  55-**************G*TN*-80  94-E****T*****T***DS*V*-113
HPV66  17-******LS****E*V*N***Q-37  55-****S***A**V***S**S*-80  94-ES***T*****T****S*V*-113
HPV68  17-*******S*****V*N****-37  55-****************GK*N*-80  94-E****TE****Q***DS*V*-113
HPV73  19-*************V*****-39  57-*****S***S*****V**S*GTPS-82  98-TS*****S*******S***-117

  P18/38 ━━━━━━━━━━━━━━━━━━━━  P56/75 ━━━━━━━━━━━━━━  P96/115 ━━━━━━━━━
                              P61/75 ━━━━━━━━━━━━━━
                               P64/81 ━━━━━━━━━
```
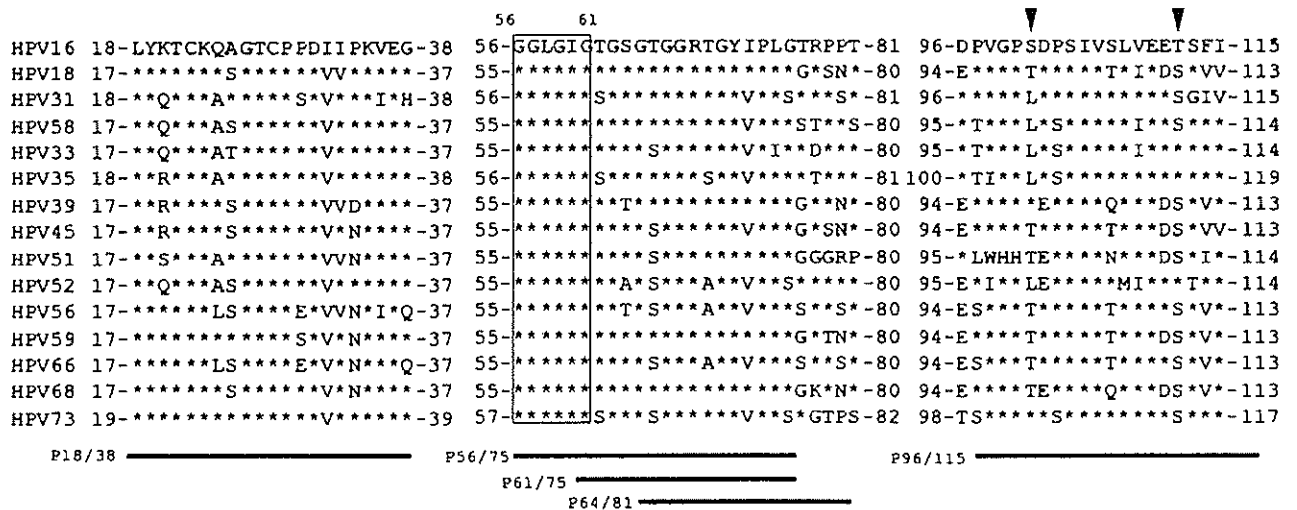
Fig. 2. Amino acids sequences of the L2 portions, aa 18 to 38, aa 56 to 81, and aa 96 to 115 of HPV16 and the corresponding portions of the other oncogenic HPVs. Amino acids identical to those of HPV16 were indicated by asterisk (*).

develop a vaccine antigen capable of inducing multiple antibodies binding to different epitopes on the L2 surface region. Since the aa sequences of the L2 surface regions of 15 oncogenic HPVs are largely similar, it seems possible to develop a vaccine antigen capable of inducing antibodies binding to the L2 surface regions of the multiple types of the oncogenic HPVs.

Materials and methods

Cell

293TT cells, a cell line expressing a high level of SV40 T antigen, was a kind gift from J. T. Schiller (National Cancer Institute, USA). The cells were cultured with in Dulbecco's modified minimal essential medium (DMEM) supplemented with 10% fetal bovine serum, 1% non-essential amino acids (Invitrogen Corp. Carlsbad, CA), 1% GlutaMax-I (Invitrogen Corp.), and hygromycine B (400 µg/ml) (Invitrogen Corp.).

Plasmids

Five plasmids; pYSEAP expressing SEAP, p16L1h expressing HPV16 L1, p16L2h expressing HPV16 L2, peL1fB expressing HPV18 L1, and peL2bhb expressing HPV18 L2 were gifts from J.T. Schiller. Four plasmids; p31L1h expressing HPV31 L1, p31L2h expressing HPV31 L2, p58L1h expressing HPV58 L1, and p58L2h expressing HPV58 L2 were newly constructed by the replacement of the HPV16L1 gene in p16L1h with the codon-modified HPV31L1, HPV31L2, HPV58L1, and HPV58L2 genes, respectively. The codons were changed to those used most frequently in human mRNAs; Ala: GCC; Cys: TGC; Asp: GAC; Glu: GAG; Phe: TTC; Gly: GGC; His: CAC; Ile: ATC; Lys: AAG; Leu: CTG; Asn: AAC; Pro: CCC; Gln: CAG; Arg; AGG; Ser: AGC; Thr: ACC; Val: GTG; Trp: TGG; Tyr: TAC.

Synthetic peptides

Peptides (Fig. 1) were synthesized by Fmoc method (SCRUM Inc., Tokyo, Japan). C was added to the N-terminus of P56/75, P61/75, P61/75(73V), P64/81, P-96/115, P96/115 (101L. 122S), and P-107/122 and to the C-terminus of P131/144, respectively. The carrier protein, keyhole limpet hemocyanin (KLH), was conjugated with P14/27 and P18/38 by bisimide-ester method. KLH was conjugated with the other peptides at the N- or C-terminus Cs of the peptides by the m-maleimidobenzoyl-N-hydroxysuccinimide-ester method.

Rabbit anti-peptide serum

The peptide was conjugated with KLH at the cysteine residue of each peptide. Japanese white rabbits (2.3–3.0 kg of weight, 2 animals for each antigen) were subcutaneously injected with the KLH conjugated peptide antigens mixed with Freund's complete adjuvant (SCRUM Inc., Tokyo, Japan). Immunization was repeated 4 times at 2-week interval, and

serum was obtained at 1 week after the last immunization. The antisera were filtered (Steradisc25, KURABO Inc., Osaka, Japan) before use for the assays in this study.

Preparation of capsids

The recombinant baculoviruses capable of expressing HPV16L1, HPV16L1/L2, HPV18L1/L2, HPV31L1/L2, HPV58L1/L2 were produced by using Bac-to-Bac baculovirus expression system (Invitrogen Corp., Carlsbad, CA), following the manufacturer's instruction. The transfer vectors pFastbac1 was used for the cloning of the L1 gene, and pFastbac dual was used for the cloning of both L1 and L2 genes. The recombinant baculovirus was inoculated to Sf9 cells (5 bottles of 175 cm^2 culture flask) and incubated for 3 days at 27 °C. The cells were collected and suspended in 5 ml of PBS containing 0.5% NP-40. After 10-min incubation at room temperature (RT), the cells were centrifuged at 10,000×g at 4 °C for 15 min to precipitate nuclei. The nuclei were suspended in PBS containing CsCl (1.28 g/ml) and lysed with brief sonication. The solution was centrifuged at 34,000 rpm at 20 °C for 20 h in an SW50.1 rotor (BECKMAN COULTER Inc., Fullrerion, CA). The fractions around a buoyant density of 1.28 g/ml were pooled and dialyzed against phosphate buffer (pH7.4) containing 0.5 M NaCl at 4 °C to remove CsCl.

ELISA with the L1 capsid of HPV16 and the L1/L2-capsids of HPV16, 18, 31, and 58 as antigens

A well of the ELISA plate was coated with 100 µl of PBS (pH 7.4) containing the purified L1 capsids (1 µg) or the L1/L2-capsids (1 µg) by incubation for 14 to 16 h at 4 °C. The well was blocked with 5% skim milk in PBS containing 0.1% Tween 20 for 2 h at 37 °C. After washing with PBS containing 0.05% Tween 20 and 0.05% NP-40 three times, 100 µl of the serum sample was added to the well and incubated for 1 h at RT. The secondary antibody was horseradish peroxidase-conjugated anti-rabbit IgG goat serum (SC-2030, Santa Cruz Biotechnology, Inc., Santa Cruz, CA). A mixture of 0.01% H$_2$O$_2$ and o-phenylenediamine (2 mg/ml) in 0.1 M citrate buffer (pH4.7) was added to the wells and the absorbency at 450 nm was measured after incubation for 30 min at 22 °C.

Preparation of pseudovirions

293TT cells, which had been seeded in a 10-cm culture dish (4 × 10^6 cells) at 16 h before the transfection, were transfected with a mixture of an L1-plasmid, an L2-plasmid, and pYSEAP by using Optifect (Invitrogen Corp.). For HPV16, 31, and 58 pseudovirion production 13.5 µg of the L1-plasmid, 3 µg of the L2-plasmid, and 13.5 µg of pYSEAP were used. For HPV18 pseudovirion production 14.5 µg of the L1-plasmid, 1 µg of the L2-plasmid, and 14.5 µg of pYSEAP were used. Sixty hours later the cells were harvested with trypsin. The cells were suspended in 0.5 ml of lysis buffer (PBS containing 1 mM CaCl$_2$, 10 mM MgCl2, 0.35% Brij58 [Sigma-Aldrich Inc., St. Louis, MO], 0.1% Benzonase [Sigma-Aldrich Inc.],

0.1% Plasmid Safe ATP dependent-DNase [EPICENTRE Corp. Madison, WI]) and incubated for 30 h at 37 °C with slow rotation. The lysate was cooled on ice for 5 min, mixed with 5 M NaCl solutions to adjust to concentration of NaCl to 0.85 M, and further kept on ice for 10 min. Then, the lysate was centrifuged at $5000 \times g$ for 10 min at 4 °C. The supernatant was laid on an Optiprep gradient (from top to bottom, 27%, 33%, and 39% in PBS containing 1 mM $CaCl_2$, 10 mM $MgCl^2$, and 0.8 M NaCl) and centrifuged at 50,000 rpm for 3.5 h at 16 °C with SW55Ti rotor (Beckman Coulter Inc. Fullerton, CA). Fractions (300 µl each) were obtained by puncturing the bottom. An aliquot (1 µl) of each fraction was inoculated to 293TT cells (2×104) in 96-well flat-bottom tissue culture treated plates (Corning Costar Corp., New York, NY). SEAP activity of the culture medium was measured by the colorimetric SEAP assay (NCI home page: http://home.ccr.cancer.gov/lco/colorimetricseap.htm). The fraction induced the highest SEAP activity in the culture medium of the cells was used for the neutralization test as a stock of the infectious pseudovirions. To remove aggregates the pseudovirion stock was filtered (Ultrafree-MC centrifugal Filter Devices, MILIPORE corp., Bedford, MA) before use for the neutralization assay.

Neutralization test

The serum was diluted with the neutralization medium (DMEM [without phenol red] containing 10% FBS, 1% non-essential amino acids, 1% GlutaMax-I). Fifty µl of a serum sample was mixed with 50 µl of the neutralization medium containing an aliquot of the pseudovirion stock (0.05 µl of HPV16, 31, and 58 pseudovirions and 0.2 µl of HPV18 pseudovirions) and incubated for 1 h at room temperature. Then, the mixture was inoculated to 293TT cells (2×10^4) that had been seeded with 100 µl of the neutralization medium in 96-well flat-bottom tissue culture plates 6 h prior to the inoculation. The culture medium was harvested after incubation of the cells for 66 h at 37 °C, and SEAP activity of the culture medium was measured by the colorimetric SEAP assay. The neutralization titer was presented as the reciprocal of maximum dilution of serum that reduced SEAP level to half of the sample not treated with serum.

Acknowledgments

References

Baker, T.S., Newcomb, W.W. Olson, N.H., Cowsert, L.M., Olson, C., Brown, J.C., 1991. Structures of bovine and human papillomaviruses: analysis by cryoelectron microscopy and three-dimensional image reconstruction. Biophys. J. 60, 1445–1456.

Breitburd, F., Kimbauer, R., Hubbert, N.L., Nonnenmacher, B., Trin-Dinh-Desmarquet, C., Orth, G., Schiller, J.T., Lowy, D.R., 1995. Immunization with viruslike particles from cottontail rabbit papillomavirus(CRPV) can protect against experimental CRPV infection. J. Virol. 69 (6), 3959–3963.

Buck, C.B., Pastrana, D.V., Lowy, D.R., Schiller, J.T., 2004. Efficient intracellular assembly of papillomaviral vectors. J. Virol. 78 (2), 751–757.

Crawford, L.V., Crawford, E.M., 1963. A comparative study of polyoma papilloma viruses. Virology 21, 258–263.

Embers, M.E., Budgeon, L.R., Pickel, M., Christensen, N.D., 2002. Protective immunity to rabbit oral and cutaneous papillomaviruses immunization with short peptides of L2, the minor capsid protein. J. Virol. 76 (19), 9798–9805.

Ferlay, J., Parkin, D.M., Pisani, P., 1998. GLOBOCAN graphical package 1. cancer incidence and mortality worldwide. IARC Press. Lyon Electronic citation.

Giroglou, T., Sapp, M., Lane, C., Fligge, C., Christensen, N.D., Streeck, R.E., Rose, R.C., 2001. Immunological analyses of human papillomavirus capsids. Vaccine. 19, 1783–1793.

Harper, D.M., Franco, D.M., Wheeler, C.M., Moscocki, A.B., Romanoswski, B., Roteli-Martins, C.M., Jenkins, D., Schuind, A., Costa Clemens, S.A., Dubin, G., 2006. HPV vaccine study group. 2006. Sustained efficacy up to 4.5 years of a bivalent L1 virus-like particle vaccine against human papillomavirus types 16 and 18: follow-up from a randomised control trial. Lancet 367 (9518), 1247–1255.

Heino, P., Skyldberg, B., Lehtinen, M., Rarotala, I., Hagmar, B., Kreider, J.W., Kimbauer, R., Dillner, J., 1995. Human papillomavirus type16 capsids expose multiple type-restricted and type common antigenic epitopes. J. Gen. Virol. 76, 1141–1153.

Jones, S.B., 1999. Cancer in the developing world: a call to action. BMJ 319, 505–508.

Kawana, K., Yoshikawa, H., Taketani, Y., Kanda, T., 1999. Common neutralizing epitope in minor capsid protein L2 of human papillomavirus Types 16 and 6. J. Virol. 73 (3), 6188–6190.

Kimbauer, R. Booy, F., Cheng, N., Lowy, D.R., Schiller, J.T., 1992. Papillomavirus L1 major capsid protein self-assembles into virus-like particles that are highly immunogenic. Proc. Natl. Acad. Sci. U.S.A. 89, 12180–12184.

Liu, W.J., Gissman, L., Sun, X.Y., Kanjanahaluethai, A., Muller, M., Doorbar, J., Zhou, J., 1997. Sequence close to the N-terminus of L2 protein is displayed on the surface of bovine papillomavirus type1 virions. Virology 227, 474–483.

Munoz, N., Bosch, F.X., Castellsague, X., Diaz, M., Sanjose, S., Hammouda, D., Shah, K.V., Meijer, C.J.L.M., 2004. Against which human papillomavirus types shall we vaccinate and screen? Int. J. Cancer 111, 278–285.

Pastrana, D.V., Gambhira, R., Buck, C.B., Pang, YY.S., Thompson, C.D., Culp, T.D., Christensen, N.D., Lowy, D.R., Schiller, J.T., Roden, R.B.S., 2005. Cross-neutralization of cutaneous and mucosal papillomavirus types with anti-sera to the amino terminus of L2. Virology 337 (2), 365–372.

Roden, R.B., Greenstone, H.L., Kimbauer, R., Booy, F.P., Jessie, J., Lowy, D.R., Schiller, J.T., 1996. In vitro generation and type-specific neutralization of a human papillomavirus type16 virion pseudotype. J. Virol. 70, 5875–5883.

Roden, R.B., Yutzy, W.H., Fallon, R., Inglis, S. Lowy, D.R., Schiller, J.T., 2000. Minor capsid protein of human genital papillomaviruses contains subdominant, cross-neutralizing epitopes. Virology 270, 254–257

Stoler, M.H. 2000. Human papillomaviruses and cervical neoplasia: a model for carcinogenesis. Int. J. Gynecol. Pathol. 19, 16–28.

Stauffer, Y., Raj, K. Masternak, K. Beard, P. 1998. Infectious human papillomavirus type18 pseudovirions. J. Mol. Biol. 283, 529–536.

Suzich, J.A. Ghim, S.J. Palmer-hill, F.J. White, W.I. Tamura, J.K. Bell, J.A. Newsome, J.A. Jenson, A.B., Schlegel, R. 1995. Systemic immunization with papillomavirus L1 protein completely prevents the development of viral mucosal papillomas. Proc. Natl. Acad. Sci. U.S.A. 92, 11553–11557.

Unckell, F., Streeck, R.E., Sapp, M., 1997. Generation and neutralization of pseudovirions of human papillomavirus type33. J. Virol. 71, 2934–2939.

Villa, L.L., Costa, R.L. Petta, C.A. Andrade, R.P., Ault, K.A., Giuliano, A.R.

Wheeler, C.M., Koutsky, L.A., Malm, C., Lehtinen, M., Skjeldestad, F.F., Olsson, S.E., Steinwall, M., Brown, D.R., Kurman, R.J., Ronnett, B.M., Stoler, M.H., Ferenczy, A., Harper, D.M., Tamms, G.M., Yu, J., Lupinacci, L., Railkar, R., Taddeo, F.J., Jansen, K.U., Esser, M.T., Sings, H.L., Saah, A.J., Barr, E., 2005. Prophylactic quadrivalent human papillomavirus (types 6, 11, 16, and 18) L1 virus-like particle vaccine in young women: a randomised double-blind placebo-controlled multicentre phase II efficacy trial. Lancet Oncol. 6 (5), 256–257.

Zhao, K.N., Sun, X.Y., Frazer, I.H., Zhou, J., 1998. DNA packaging by L1 and L2 capsid proteins of bovine papillomavirus type 1. Virology 243, 482–491.

Zhou, J., Sun, X.Y., Stenzel, D.J., Frazer, I.H., 1991. Expression of vaccinia recombinant HPV16L1 and L2 ORF proteins in epithelial cells is sufficient for assembly of HPV virion-like Particles. Virology 185, 251–257.

Zhou, J., Stenzel, D.J., Sun, X.Y., Frazer, I.H., 1993. Synthesis and assembly of infectious bovine papillomavirus particles in vitro. J. Gen. Virol. 74, 763–768.

CD1d Degradation in *Chlamydia trachomatis*-infected Epithelial Cells Is the Result of Both Cellular and Chlamydial Proteasomal Activity[*]

Kei Kawana[+§], Alison J. Quayle[¶], Mercedes Ficarra[¶], Joyce A. Ibana[¶], Li Shen[∥], Yukiko Kawana[+], Huixia Yang[§¶], Luis Marrero[**], Sujata Yavagal[§], Sheila J. Greene[¶], You-Xun Zhang[∥], Richard B. Pyles[++], Richard S. Blumberg[§§], and Danny J. Schust[+1]

From the [+]Division of Reproductive Biology, Department of Obstetrics and Gynecology, Boston Medical Center, Boston University School of Medicine, Boston, Massachusetts 02118, the [§]Department of Obstetrics, Gynecology and Reproductive Biology, Brigham and Women's Hospital, Harvard Medical School, Boston, Massachusetts 02115, the [¶]Department of Microbiology, Immunology, and Parasitology, Louisiana State University Health Sciences Center, New Orleans, Louisiana 70112, the [∥]Division of Infectious Diseases, Department of Medicine, Boston University School of Medicine, Boston, Massachusetts 02118, the [**]Gene Therapy Program, Louisiana State University Health Sciences Center, New Orleans, Louisiana 70112, the [++]Department of Pediatrics and Experimental Pathology, Sealy Center for Vaccine Development, University of Texas Medical Branch, Galveston, Texas 77555, and the [§§]Division of Gastroenterology, Department of Medicine, Brigham and Women's Hospital, Harvard Medical School, Boston, Massachusetts 02115

Chlamydia trachomatis is an obligate intracellular pathogen that can persist in the urogenital tract. Mechanisms by which *C. trachomatis* evades clearance by host innate immune responses are poorly described. CD1d is MHC-like, is expressed by epithelial cells, and can signal innate immune responses by NK and NKT cells. Here we demonstrate that *C. trachomatis* infection down-regulates surface-expressed CD1d in human penile urethral epithelial cells through proteasomal degradation. A chlamydial proteasome-like activity factor (CPAF) interacts with the CD1d heavy chain, and CPAF-associated CD1d heavy chain is then ubiquitinated and directed along two distinct proteolytic pathways. The degradation of immature glycosylated CD1d was blocked by the proteasome inhibitor lactacystin but not by MG132, indicating that degradation was not via the conventional proteasome. In contrast, the degradation of non-glycosylated CD1d was blocked by lactacystin and MG132, consistent with conventional cellular cytosolic degradation of *N*-linked glycoproteins. Immunofluorescent microscopy confirmed the interruption of CD1d trafficking to the cell surface, and the dislocation of CD1d heavy chains into both the cellular cytosol and the chlamydial inclusion along with cytosolic CPAF. *C. trachomatis* targeted CD1d toward two distinct proteolytic pathways. Decreased CD1d surface expression may help *C. trachomatis* evade detection by innate immune cells and may promote *C. trachomatis* persistence.

Chlamydia trachomatis serovars D–K are common obligate intracellular pathogens that infect the columnar epithelia of the human urogenital mucosa (1, 2). Infection most frequently occurs in the penile urethra or endocervix and causes acute inflammatory responses at these sites (1–3). Despite immune recognition of infection, *C. trachomatis* can persist within the host, and persistence is associated with more severe disease (2, 3). *C. trachomatis*-associated alterations in host immunity are thought to promote persistence, and these immunoevasive mechanisms may affect innate immune responses, adaptive immune responses, or both.

Mechanisms for evasion of adaptive responses by *C. trachomatis* have been described, including the down-regulation of MHC[2] class I heavy chain (HC) and β2-microglobulin (β2m) expression (4–7). Down-regulation appears to be the result of a novel chlamydial proteasome-like activity factor (CPAF) (4, 6). CPAF, composed of N-terminal (29 kDa) and C-terminal (35 kDa) fragments, is secreted from the chlamydial inclusion into the host cytosol and degrades the transcriptional factor RFX5 that would otherwise up-regulate promoters of MHC class I HC and β2m genes (4, 6). *C. trachomatis* also targets upstream stimulation factor-1 for CPAF-mediated degradation, resulting in the inhibition of interferon γ-inducible expression of MHC class II products (5). Cellular fractionation places CPAF into subfractions that differ from those containing the classic cytosolic proteasome subunits. Further, CPAF-associated proteasomal activity is inhibited by one cytosolic proteasome inhibitor, lactacystin, but not by other proteasome inhibitors (4, 6). These data indicate that CPAF has proteasomal activities distinct from those of the classic cytosolic proteasome.